Management Science

Publication details, including instructions for authors and subscription information:
http://pubsonline.informs.org

The Normalization of Consumer Valuations: Context-Dependent Preferences from Neurobiological Constraints

Ryan Webb, Paul W. Glimcher, Kenway Louie

To cite this article:
Ryan Webb, Paul W. Glimcher, Kenway Louie (2021) The Normalization of Consumer Valuations: Context-Dependent Preferences from Neurobiological Constraints. Management Science 67(1):93-125. https://doi.org/10.1287/mnsc.2019.3536

http://pubsonline.informs.org/journal/mnsc

MANAGEMENT SCIENCE
Vol. 67, No. 1, January 2021, pp. 93–125
ISSN 0025-1909 (print), ISSN 1526-5501 (online)

The Normalization of Consumer Valuations: Context-Dependent Preferences from Neurobiological Constraints

Ryan Webb,[a] Paul W. Glimcher,[b] Kenway Louie[c]

[a] Rotman School of Management, University of Toronto, Toronto, Ontario M5S 3E6, Canada; [b] Department of Neuroscience and Physiology, Langone School of Medicine, New York University, New York, New York 10016; [c] Center for Neural Science, New York University, New York, New York 10016

Contact: ryan.webb@utoronto.ca, https://orcid.org/0000-0003-0035-7037 (RW); pg3@nyu.edu (PWG); kl837@nyu.edu, https://orcid.org/0000-0002-9665-5436 (KL)

Received: May 3, 2017
Revised: July 18, 2018; May 16, 2019; September 30, 2019
Accepted: September 3, 2019
Published Online in Articles in Advance: May 27, 2020

https://doi.org/10.1287/mnsc.2019.3536

Abstract. Consumer valuations are shaped by choice sets, exemplified by patterns of substitution between alternatives as choice sets are varied. Building on recent neuroeconomic evidence that valuations are transformed during the choice process, we incorporate the canonical *divisive normalization* computation into a discrete choice model and characterize how choice behaviour depends on both size and composition of the choice set. We then examine evidence for such behaviour from two choice experiments that vary the size and composition of the choice set. We find that divisive normalization more accurately captures observed behaviour than alternative models, including an example *range normalization* model. These results are robust across experimental paradigms. Finally, we demonstrate that Divisive Normalization implements an efficient means for the brain to represent valuations given neurobiological constraints, yielding the fewest choice errors possible given those constraints.

History: Accepted by Elke Weber, judgment and decision making.
Funding: This work was supported by the Army Research Office [Grant W911ND-11-1-0482].

Keywords: neuroeconomics • discrete choice • bounded rationality • divisive normalization • independence of irrelevant alternatives

1. Introduction

Consider a single bar of chocolate. In the study of consumer choice, it is typically assumed that a consumer has a valuation of said chocolate bar and that this valuation can be measured (say, by a willingness-to-pay mechanism or a rating scale). Whereas any number of factors might determine a consumer's valuation, like the amount, type, or "nuttiness" of the chocolate, a standard assumption is that this valuation is stable; when faced with a variety of other alternative chocolate bars, the consumer's choice is determined by their willingness to pay for each item individually. In this article, we study how consumer valuations might be shaped by the composition of the choice set.

How consumer preferences depend on the elements of a choice set, and why they might differ from a strictly rational benchmark, has long been of interest to behavioural science. A long literature demonstrates systematic inconsistency between independent willingness-to-pay measures and the valuations implied from choices between pairs of alternatives (Slovic and Lichtenstein 1983). This has led to the suggestion that preferences are typically constructed at the time of choice rather than simply stored, retrieved, and compared (Lichtenstein and Slovic 2006, Weber and Johnson 2009). The process by which this value information is accumulated and compared in a decision can bias preferences toward an alternative simply because of the constraints involved in simultaneously processing information about both choice alternatives (Krajbich et al. 2010, Polania et al. 2019).

An early sufficient condition for stochastic choice models held that relative preferences (i.e., relative choice probabilities) between any two alternatives should be independent of all others, formally stated as the axiom of Independence of Irrelevant Alternatives (IIA; Luce 1959). This axiom served as a benchmark, because, if IIA is satisfied, it is sufficient to represent a decision-maker's preferences with a *random utility* and analyze their choice behaviour with the familiar Multinomial Logit model (see McFadden 2001 for a review).[1] Not surprisingly, IIA places strong conditions on behaviour (Debreu 1960), and violations have been well-documented empirically at both the population and individual level (Rieskamp et al. 2006). These violations consist of substitution patterns between alternatives as the composition of the choice set is varied.

Some forms of IIA violations can be rationalized by placing different distributional assumptions on the random utility representation (Train 2009). These rationalizations include allowing the variance of a random

utility to depend on the composition of the choice set, an issue particularly critical to analyzing consumer choice data in both the laboratory and field (Louviere et al. 2002, Salisbury and Feinberg 2010). However, this modelling approach is — by definition — agnostic about the process by which decisions are made. A tighter link between the choice model and the brain's decision process might lead to a more precise specification of the variance, thus a better performing model. In this article, we leverage recent neurobiological evidence to model how valuations are transformed and compared in the decision-making process. Similar to perceptual systems in the brain, we focus on the role of neurobiological constraints in shaping the valuations of choice alternatives according to a neural computation called *Divisive Normalization*. Embedded within a discrete choice model, Divisive Normalization shapes the substitution patterns that violate IIA.

1.1. Neurobiological Constraints on Choice

The observation that biology influences choice behaviour is not novel (Robson 2001a, Robson and Samuelson 2010, Netzer 2009, Glimcher 2011, Alonso et al. 2014). This includes the observation that a constrained decision process implies behaviour we might strictly term irrational ex ante but is, in fact, an optimal response to some constraint (Simon 1979).[2] Like constraints traditionally described in economics, neurobiological constraints arise from scarcity; neurons require energy in order to transmit information and resources must be allocated to various neural systems for various tasks. This fundamental constraint has two important implications for neural computation, which we briefly describe here. A deeper survey can be found in Appendix A.

Neural Activity Is Stochastic. Stochasticity in neural activity arises, at least in part, from the small-scale thermodynamic processes involved in the transmission of information between neurons (Mainen and Sejnowski 1995, Stevens 2003, Glimcher 2005). Increasing the number (or size) of neurons that participate in a computation can only partially mitigate this stochasticity (Shadlen and Newsome 1998) and is costly in terms of resources. Ultimately, this stochasticity influences the discriminability of quantities encoded by neural activity, yielding a degree of stochastic behaviour (Glimcher 2005).

The Brain Encodes Information in Relative Terms. The relative coding of information by neural systems is one of the fundamental observations of neuroscience in the past century (Hartline and Ratliff 1957). Because neural activity is bounded — in terms of the dynamic range of a single neuron and the finite number of neurons in a brain area — computational algorithms have evolved that efficiently compress the objective state of the world for subjective perception. On the retina, for example, light intensity is encoded relative to average ambient illumination; this process of light adaptation is why black type on white newspaper appears the same in a darkened room and under bright sunlight, even though the newsprint may reflect up to 6 orders of magnitude more photons in the latter environment. This relative representation of information is observed to be a general feature of sensory coding (Carandini and Heeger 2012), and more recently, has been observed in the neural computations of value information (for reviews, see Glimcher 2003, Seymour and McClure 2008, Rangel and Clithero 2012, Louie et al. 2015).

Our contribution is to examine *how* choice-set dependence arises in a decision process that obeys neurobiological constraints and to formally test predictions on what form it will take. We consider a bounded function which is tasked with identifying the highest-valued alternative in a choice set. Formally, Robson (2001b) and Rayo and Becker (2007) first considered the properties of such a function given that (i) the limited perception of small differences in value, and (ii) the value function is bounded above and below.[3] For guidance on the form of this function and its role in shaping valuations during the decision process, we turn to the neurobiological evidence.

1.2. Divisive Normalization

Divisive Normalization is a pervasive computation in cortex that implements a relative coding of information (Carandini et al. 1997, Schwartz and Simoncelli 2001). Originally observed in the cortical regions of the brain involved in visual perception (Heeger 1992), divisive normalization has been documented across sensory modalities and across species ranging from invertebrates to primates (Carandini and Heeger 2012). More recently, evidence for normalization has been observed in the neural computation of valuations while subjects evaluate potential choice alternatives: The neural activity associated with the value of a choice object is suppressed by the valuation and number of other alternatives (Louie et al. 2011, Holper et al. 2017). We review this empirical literature in more detail in Appendix A.2.

Divisive Normalization is a simple neural computation that can be implemented by only a few neurons in a cortical circuit; mathematically, it can be represented by a function that scales, or normalizes, its inputs (Louie et al. 2014, LoFaro et al. 2014). Consider first a simplified form of the Divisive Normalization function,

$$z_i(\mathbf{v}) = \frac{v_i}{\|\mathbf{v}\|_\beta}, \tag{1}$$

where each element of an input vector $\mathbf{v}=[v_1,\ldots,v_N]\in\mathbb{R}_+^N$ is scaled by the magnitude and number of its elements by a norm of degree β, denoted $\|\mathbf{v}\|_\beta \equiv (\sum_{n=1}^{N} v_n^\beta)^{\frac{1}{\beta}}$. If we take the inputs v_i to represent some independent valuation of an alternative i, and $z_i(\mathbf{v})$ to represent the transformation of each alternative in a choice set at the time of decision, then each alternative is normalized with respect to the entire vector of alternatives.[4] This yields a bounded valuation $z_i(\mathbf{v})$ with a relative relationship between alternatives.

To establish both the positive and normative implications of Divisive Normalization, in Section 3 we incorporate a general form of Equation (1) directly within a discrete choice model and demonstrate how choice probabilities depend on the size and composition of the choice set. Previous work has demonstrated that a simple form of normalization (with $\beta = 1$) is qualitatively consistent with violations of the IIA axiom (Louie et al. 2013). Here, we fully characterize the substitution patterns that arise from a general form of Equation (1) when adding and altering alternatives in the choice set. We demonstrate how this general formulation can be estimated and tested formally with discrete choice data, how it incorporates some existing forms of normalization as a special case, and contrast its predictions with alternative models.

For example, Divisive Normalization predicts a decrease in the likelihood of choosing a high-valued alternative as low-valued alternatives are added or manipulated. Consider two alternatives that, when evaluated independently, have valuations $v_1 > v_2 \geq 0$. Under Divisive Normalization, introducing a third alternative $v_3 < v_2$ to this choice set shrinks the difference between $z_1(\mathbf{v}) - z_2(\mathbf{v})$. This gap shrinks farther as the value of this third alternative increases or as more lower-valued alternatives are added. Provided a stochastic model in which choice probabilities depend on valuation differences, normalization therefore predicts how the probability of choosing the highest-valued alternative depends on the set of alternatives (Steverson et al. 2019). This yields novel forms of IIA violations and choice probabilities compatible with Weber scaling (Weber 1834) and imposes a precise specification for how the variance of the model differs over choice sets.

However, even in the absence of normalization, it is not immediately clear that a random utility model cannot capture such substitution patterns. Whereas the Multinomial Logit obviously predicts no IIA violations as v_3 is altered, the flexible Multinomial Probit (MNP) formulation can capture a wide variety of substitution patterns, thus it may outperform a model with Divisive Normalization. As we describe below, an alternative form of normalization that scales valuations by their range rather than their sum (Soltani et al. 2012, Bushong et al. 2019) makes an opposite prediction about the substitution pattern as v_3 is varied.

To sort between these different explanations, in Section 4 we estimate and test the predictions of a general normalization model in two behavioural experiments: one previously reported trinary choice experiment that varies the composition of the choice set (Louie et al. 2013) and a second novel experiment that varies the size of the choice set. Importantly, our modelling approach nests competing accounts for IIA violations. We find strong evidence for Divisive Normalization; neither the MNP nor Range Normalization are able to capture the substitution patterns we observe. Our structural specification also provides an estimate for the degree of normalization β that is larger than the simple form (with $\beta = 1$), and we find evidence that recurrent connections are more strongly weighted in the normalization equation then all others.

Our structural approach to model testing has one other advantage: The resulting estimates of normalization parameters can be used to examine the robustness of each model.[5] Our second experiment, conducted on a separate subject sample, therefore allows us to assess each model's performance in a strict out-of-sample prediction exercise. Notably, the estimates from the Divisive Normalization model in the trinary choice experiment provide a good prediction of the choice probabilities in the second experiment that varies the size of the choice set; this out-of-sample prediction performs better than both a standard Probit and a Range Normalization model fit in-sample.

From a normative standpoint, Divisive Normalization has also been shown to yield an efficient coding of sensory information in a constrained neural system (Schwartz and Simoncelli 2001, Wainwright et al. 2001, Sinz and Bethge 2013, Qamar et al. 2013). However, the normative implications for choice behaviour have remained unclear, particularly because Divisive Normalization predicts a decrease in the likelihood of choosing a higher-valued alternative as low-valued alternatives are manipulated or as the choice set is expanded (up to 20% in the largest choice sets in our experiment). In the absence of constraints, such behaviour can be strictly termed inefficient. However, given neurobiological constraints, Divisive Normalization implements choice behaviour that is optimal (in the sense of minimizing choice errors).[6] We thus offer one explanation for why — at a neurobiological level — boundedly rational behaviours exist. Taken all together, these results emphasize both the positive and normative advances offered by developing choice models grounded in neuroscience.

2. Model

To highlight the role of normalization in shaping valuations during a decision, we present a simple "two-stage"

model of decision-making (Fehr and Rangel 2011, Glimcher 2011, Webb et al. 2019). The distinction between these stages lies in brain regions that aggregate value information in a choice-independent manner and those that employ that value information in the process of choice (Platt and Plassmann 2013, Polania et al. 2015). Here, we adopt this two-stage model to demonstrate how the Divisive Normalization computation shapes valuations in a discrete choice model. For a more nuanced discussion of the empirical literature underlying this modelling approach, see Appendix A.3.

We begin by defining a quantity called *subjective value* that carries information about the valuations of each alternative in a choice set of size N. These valuations are denoted by the vector $\mathbf{v} = [v_1, \ldots, v_N] \in \mathbb{R}^N_+$, where v_i is the valuation of each alternative $i \in \{1, \ldots, N\}$. Without loss of generality, we assume that the first alternative has largest valuation, so $v_1 > v_j, \forall j \neq 1$. To isolate the behavioural implications of Divisive Normalization, we will assume that a particular observation of $\mathbf{v}$ has been realized and is thus deterministic in the subsequent analysis. In our empirical analysis, we measure this valuation with a standard willingness-to-pay mechanism independently for each item (Becker et al. 1964).[7]

We note that our definition of subjective value is general enough to incorporate a range of discrete choice models that take observable attributes as arguments. For instance, a realization of $\mathbf{v}$ can be constructed via a behavioural theory linking different attributes $\mathbf{x}$ to valuations, $\mathbf{v} = V(\mathbf{x})$, whether those attributes are defined either objectively as sensory input or only latently (Bhatia and Stewart 2018). We strongly suspect that the brain implements relative coding in earlier stages of the decision-making process — for instance, in the construction of $\mathbf{v}$. The existence of some form of relative coding in attribute integration essentially follows both from the results of Rayo and Becker (2007) and the neurobiological evidence for sensory systems (see Appendix A.1). Here, we restrict our attention to analyzing "value normalization" that has been empirically documented in regions of the primate brain (see Appendix A.2). We do so to provide a parsimonious account of the role of neurobiological constraints — and normalization, in particular — in predicting context-dependent choice patterns beyond the multiattribute domain typically studied. In recent work, extending normalization to the multiattribute domain, Landry and Webb (2020) address a range of phenomena including well-known decoy effects that rely on a particular structure of numerically presented attributes (Tversky 1972, Huber et al. 1982, Simonson 1989).[8]

The second stage of the model involves the comparison of subjective value for the purpose of choice. This is where we will explore the implications of neurobiological constraints for inducing context-dependent choice behaviour. Instead of assuming that independent ("context-free") valuations are compared in this second stage, we consider a function that maps the valuations of all alternatives in the choice set into a common, bounded, region of neural activity for comparison. Formally, we define $z(\mathbf{v}) : \mathbb{R}^N_+ \to Z$, which maps $\mathbf{v}$ to a vector $[z_1(\mathbf{v}), \ldots, z_N(\mathbf{v})]$ in a compact subspace $Z \equiv [0, \bar{z}]^N \subset \mathbb{R}^N_+$. The bound constraint is therefore given by $0 < \bar{z} < \infty$.

In Section 2.1, we will examine the role of the divisive normalization function

$$z_i(\mathbf{v}) = \frac{v_i}{\sigma + \omega\left(\sum_n v_n^\beta\right)^{\frac{1}{\beta}}} \tag{2}$$

in implementing the bound constraint $\bar{z}$. In this general formulation, the parameter σ determines how neural activity saturates with increased input and can be interpreted as the baseline activity level of neurons in the normalization — a form of reference point (Louie et al. 2015, Tymula and Glimcher 2019). The weight ω determines the contribution to the normalization from other alternatives. If $\omega = 0$, there is no normalization.

Finally, the choice process is modelled by the decision vector $\mathbf{u} = z(\mathbf{v}) + \boldsymbol{\eta}$, which appends a stochastic term $\boldsymbol{\eta} = [\eta_1, \ldots, \eta_N] \in \mathbb{R}^N$ to the normalized valuations. The decision-maker chooses option i when

$$\begin{aligned} u_i &> u_j, \quad \forall j \neq i \\ z_i(\mathbf{v}) + \eta_i &> z_j(\mathbf{v}) + \eta_j, \quad \forall j \neq i, \end{aligned} \tag{3}$$

yielding a probability of choosing i,

$$P_i(z(\mathbf{v})) = \int \mathbb{1}\left[z_i(\mathbf{v}) - z_j(\mathbf{v}) > \eta_j - \eta_i, \quad \forall j \neq i\right] f(\boldsymbol{\eta}) d\boldsymbol{\eta}, \tag{4}$$

which depends on the probability density function $f(\boldsymbol{\eta})$.[9]

We therefore interpret $\mathbf{v}$ as a decision-maker's independent valuation of a consumer good, and we study the choice behaviour implied when these valuations are normalized, via $z(\mathbf{v})$, in the implementation of a decision.

2.1. Implementing the Bound Constraint via Normalization

Upon initial consideration, a range of possible constraints on the allocation of neural activity are possible. Most leniently, the neural activity of each alternative could be non-rivalrous; any activity levels $z(\mathbf{v}) \in Z$ could be feasible. This is the constraint depicted in Figure 1, where each $z_i(\mathbf{v}) \leq \bar{z}$. At the other extreme, the neural activity could be perfectly rivalrous,

Figure 1. (Color online) Transformation $z(\mathbf{v})$ for Binary Choice

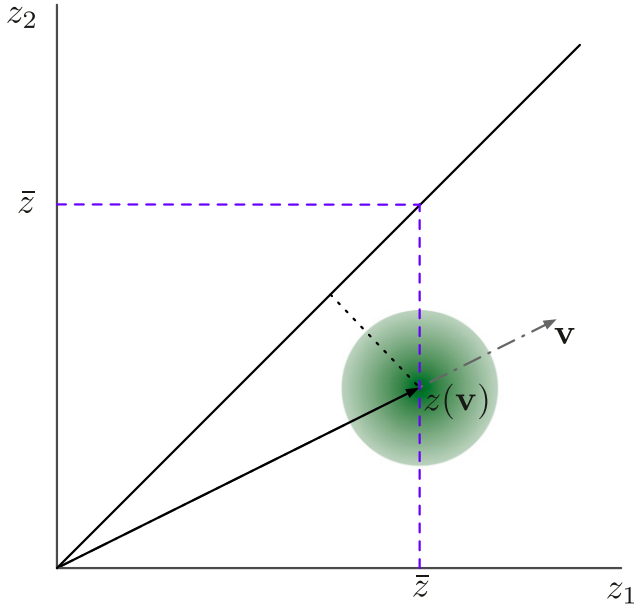

Notes. The stochasticity in the comparison $\boldsymbol{\eta}$ is depicted by the shaded error density. Therefore, the distance from the vector to the 45° line determines the probability that the alternative with the highest value is chosen, $\Pr[u_1 > u_2]$.

resulting in the linear constraint $\sum_i z_i(\mathbf{v}) \leq \bar{z}$. Of course, a nonlinear constraint can lie between these two extremes.

The critical feature of Divisive Normalization is that it scales neural activity to the boundary of these possible constraints, depending on the form of the normalization. For exposition, we present these results for the simple form of normalization given in Equation (2) with $\sigma = 0$. In our empirical results in Section 4, we will consider more general forms. Appendix E explores the implications of relaxing this assumption on σ in more detail.

We begin with the linear constraint. If $\beta = 1$, then the normalization function $z(\mathbf{v})$ scales the vector $\mathbf{v}$ along a ray to the origin, proportioning neural activity between the alternatives along the line:

$$\bar{z} = \sum_i z_i(\mathbf{v}) = \sum_i \frac{v_i}{\omega \sum_i v_i} = \frac{1}{\omega}. \tag{5}$$

We now can reinterpret the bound $\bar{z}$ as the ratio $1/\omega$, with ω determining the strength of the normalization (Figure 2). As $\omega \to 0$, the normalization term shrinks and along with it the means to bound $z(\mathbf{v})$.

For any $\beta > 0$, divisive normalization maps $\mathbf{v}$ to a general class of geometric figures known as a *superellipse*. For instance, when $\beta = 2$, normalization scales the vector $\mathbf{v}$ to the quarter-circle of radius $1/\omega$, because $z(\mathbf{v}) = \frac{1}{\omega}\frac{\mathbf{v}}{\|\mathbf{v}\|}$. Setting $\beta = 3$ maps $\mathbf{v}$ to a hyperellipse, whereas $\beta = \infty$ maps to the square of size $1/\omega$ (see Figure 1). Notice that in each of these cases, Divisive Normalization preserves the relative magnitudes of the elements of $\mathbf{v}$ and scales neural activity to the boundary determined by $\bar{z}$. Therefore, Divisive Normalization implements a relative coding of value, subject to the boundary constraint on neural activity. In the following sections, we will explore the patterns in choice behaviour generated by this relative coding of valuations.

3. Behavioural Implications of Normalization

The behavioural predictions of normalization stem from the interaction between scale and stochasticity that is typically present in discrete choice models (McFadden 2001, Train 2009). To explore these predictions, we incorporate the normalization Equation (2) directly into Equation (4):

$$P_i(z(\mathbf{v})) = \int \mathbb{1}\left[\frac{v_i - v_j}{\sigma + \omega\left(\sum_n v_n^\beta\right)^{\frac{1}{\beta}}} > \eta_j - \eta_i, \quad \forall j \neq i\right] f(\boldsymbol{\eta}) d\boldsymbol{\eta}. \tag{6}$$

In a model without normalization ($\omega = 0$), choice probabilities are given by a standard random utility formulation; thus, the scale of the model is set by the variance of the stochastic term $\boldsymbol{\eta}$. For instance, when $f(\boldsymbol{\eta})$ is the density of the independent normal distribution, $\mathrm{Var}(\eta_i)$ is typically assumed to be 1, and the parameter σ determines the variance of a binary Probit model: $\Pr[v_i - v_j > \sigma(\eta_j - \eta_i)]$. Note that this variance is constant over choice sets.

By contrast, introducing normalization scales the variance in a systematic manner proportional to the number and value of the alternatives in the choice set. This scaling depends on assumptions placed on the density $f(\boldsymbol{\eta})$, but for now, we simply maintain the standard assumption that $\mathrm{Var}(\eta_i)$ is a constant. In an important respect, a distributional specification is also what we are proposing here. If one multiplied the denominator of the normalization Equation (6) through to the right-hand side of the inequality, the distribution of the error $\boldsymbol{\eta}$ could be appropriately redefined to incorporate normalization with the inequality in brackets in Equation (6) given by

$$\left[v_i - v_j > \left(\sigma + \omega\left(\sum_n v_n^\beta\right)^{\frac{1}{\beta}}\right)(\eta_j - \eta_i)\right].$$

Therefore, value normalization is equivalent to specifying that the variance of the stochastic term in a discrete choice model depends on magnitudes in a particular manner. Recall that $i = 1$ denotes the highest valued alternative of a choice set. The following proposition states how the probability of choosing this alternative, P_1, decreases in the magnitude of the valuations.

Figure 2. (Color online) Proportionate Scaling Implemented by Normalization for (left) $\beta = 1$ and (right) $\beta = 2$

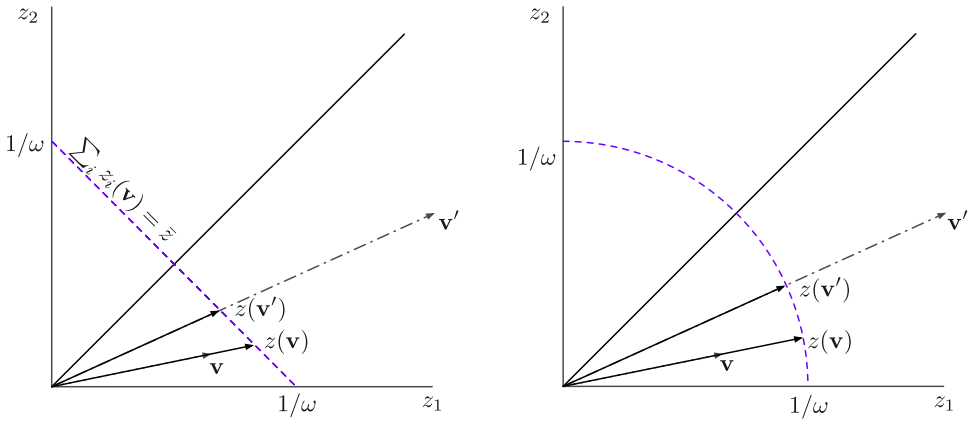

Proposition 1 (Choice Stochasticity Scales with Valuations). *For all* $\mathbf{v}$ *and* $\mathbf{v}'$ *such that* $v_i - v_j = v'_i - v'_j$, *and* $v'_i > v_i$, $\forall i, j$, *a normalized value function* (2) *implies that* $P_1(z(\mathbf{v}')) < P_1(z(\mathbf{v}))$.

Proof. From Equation (2),

$$\left|z_i(\mathbf{v}') - z_j(\mathbf{v}')\right| = \left|\frac{v'_i - v'_j}{\sigma + \omega\left(\sum_i v_i'^{\beta}\right)^{\frac{1}{\beta}}}\right| = \left|\frac{v_i - v_j}{\sigma + \omega\left(\sum_i v_i'^{\beta}\right)^{\frac{1}{\beta}}}\right| < \left|z_i(\mathbf{v}) - z_j(\mathbf{v})\right|.$$

Moreover, for the highest-valued alternative,

$$\mathbb{1}\left[z_1(\mathbf{v}') - z_j(\mathbf{v}') > \eta_j - \eta_1\right] \leq \mathbb{1}\left[z_1(\mathbf{v}) - z_j(\mathbf{v}) > \eta_j - \eta_1\right], \forall \boldsymbol{\eta} \text{ and } \forall j \neq 1.$$

Therefore, $P_1(z(\mathbf{v}')) < P_i(z(\mathbf{v}))$ from Equation (4). □

Some intuition for this scaling and its effect on choice behaviour can be observed in Figure 3. Consider two binary choice sets in which the difference between the valuations in each set are constant ($v_1 - v_2 = v'_1 - v'_2$), but the alternatives in one set are of higher value (i.e., $v'_i > v_i$). In an additive random utility model, the resulting choice probabilities in these two choice sets are equivalent (i.e., the vectors $\mathbf{v}$ and $\mathbf{v}'$ are equidistant from the 45° line). However, under normalization, there is now an important distinction, the higher-valued alternative in each set is scaled more (in absolute terms) than the lower. Therefore, the normalized valuations have a smaller *relative* ratio in the higher-valued choice set — $z(\mathbf{v}')$ is closer to the 45° line than $z(\mathbf{v})$ — leading to increased choice errors.

A dependence between choice errors and the magnitudes of stimuli — not just their differences — has been routinely described in the psychology literature for nearly two centuries, codified as Weber's law (Weber 1834, Stevens 1961, Glimcher 2011).[10] In our model, such behaviour results directly from a constrained neural computation. However, the departure of choice behaviour from a purely rational benchmark (of no choice errors) is implemented in a constrained-optimal manner.

Figure 3. (Color online) (Left) Choice Stochasticity Scales with Value of the Choice Set and (Right) Divisive Normalization Scales $\mathbf{v}$ to the Bound Constraint $\bar{z}$

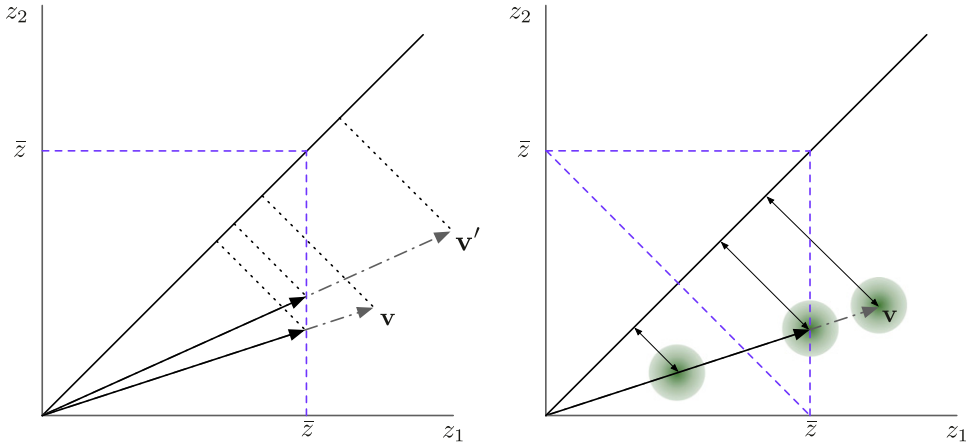

Note. Compare the scaling of $\mathbf{v}$ to the bound $\bar{z}$ versus a scaling to the interior of the bound.

Proposition 2 (Divisive Normalization with $\sigma = 0$ Yields as Few Choice Errors as Possible)**.** *For any* $\mathbf{v}$, $\bar{z}$, *and* $\alpha \in [0, \ldots, \frac{\bar{z}}{\|\mathbf{v}\|_\gamma}]$, *where* $\gamma \in [1, \ldots, \infty]$, *then* P_1 *is maximal when* $\alpha\mathbf{v}$ *is the normalized value function* (2) *with* $\omega = \frac{1}{\bar{z}}$, $\sigma = 0$, *and* $\beta = \gamma$.

The proof is provided graphically in Figure 3. Because Divisive Normalization scales $\mathbf{v}$ directly to the bound constraint, not to some interior point, the distance between the vector $z(\mathbf{v})$ and the 45° line is as large as possible. Therefore, given the bound constraint, the probability of making an error is reduced as much as possible. This result also clarifies the normative implications of β. When $\beta = 1$, normalization maps the vector $\mathbf{v}$ to a linear constraint, whereas $\beta > 1$ maps $\mathbf{v}$ to a more lenient constraint. The smallest possible probability of an error occurs when $\beta = \infty$ and $\mathbf{v}$ is mapped to a constraint given by a square.[11]

3.1. Substitution Patterns and Violations of IIA

We now consider the patterns in choice behaviour when more alternatives are introduced into the choice set. Under Divisive Normalization, the neural activity for each alternative is rescaled to abide by the bound constraint, proportionate to the value of new alternatives. Figure 4 depicts this result graphically for the addition of a third alternative (v_3) under the assumption of a linear constraint (i.e., a simplex in $\mathbb{R}^3_+$). As before, the highest-valued alternative is scaled more than the second; therefore, the difference between $z_1(\mathbf{v})$ and $z_2(\mathbf{v})$ shrinks. This scaling continues as the value of the third alternative is increased.

This pattern holds for choice sets of size N. For any choice set with valuations $\mathbf{v} \in \mathbb{R}^N_+$, define $\mathbf{v}_v \equiv [\mathbf{v}, v] \in \mathbb{R}^{N+1}_+$ as the valuation of a choice set which appends an alternative with valuation v.

Lemma 1. *A normalized value function* (2) *implies* $|z_i(\mathbf{v}_{v'}) - z_j(\mathbf{v}_{v'})| < |z_i(\mathbf{v}_v) - z_j(\mathbf{v}_v)| < |z_i(\mathbf{v}) - z_j(\mathbf{v})|$, *for all* $i, j \le N$, $j \neq i$, *all* $v' > v$, *and all* N.

Proof. By definition, $\mathbf{v}_0 = [\mathbf{v}, 0]$ is the original vector $\mathbf{v}$ but in $\mathbb{R}^{N+1}_+$. For any $N \ge 2$, and all elements $i, j \le N$,

$$\begin{aligned}
|z_i(\mathbf{v}_{v'}) - z_j(\mathbf{v}_{v'})| &= \left| \frac{v_i - v_j}{\sigma + \omega\left(v'^\beta + \sum_n^N v_n^\beta\right)^{\frac{1}{\beta}}} \right| \\
&< \left| \frac{v_i - v_j}{\sigma + \omega\left(v^\beta + \sum_n^N v_n^\beta\right)^{\frac{1}{\beta}}} \right| = |z_i(\mathbf{v}_v) - z_j(\mathbf{v}_v)| \\
&< \left| \frac{v_i - v_j}{\sigma + \omega\left(0 + \sum_n^N v_n^\beta\right)^{\frac{1}{\beta}}} \right| = |z_i(\mathbf{v}_0) - z_j(\mathbf{v}_0)|. \quad \square
\end{aligned}$$

The scaling described in Lemma 1, where the difference between normalized valuations shrinks, is a critical feature of Divisive Normalization: It implies a decrease in the odds that alternative 1 is chosen relative to alternative 2 (i.e., the ratio $\frac{P_1}{P_2}$ decreases). Therefore, substitution patterns induced by normalization depart from the IIA axiom in a testable manner.

To understand how, consider a model without normalization (i.e., $\omega = 0$ in Equation (6)). In this random utility model, substitution patterns are determined by the distribution of the error vector $\boldsymbol{\eta}$. For instance, when η_i follow the independent *Gumbel* distribution, we have the familiar Multinomial Logit (MNL) model with $P_i = \frac{e^{v_i}}{\sum_n e^{v_n}}$. The ratio $\frac{P_i}{P_j} = e^{v_i - v_j}$ does not depend on the valuations of the additional alternatives in the choice set, therefore satisfies IIA. By contrast, normalization predicts a decrease in the odds $\frac{P_1}{P_2}$, and this decrease is present even when the

Figure 4. (Color online) Introduction of a Third Alternative Scales the Valuations via the Normalization Equation and Alters the Relative Likelihood of Choosing Between Alternatives 1 and 2

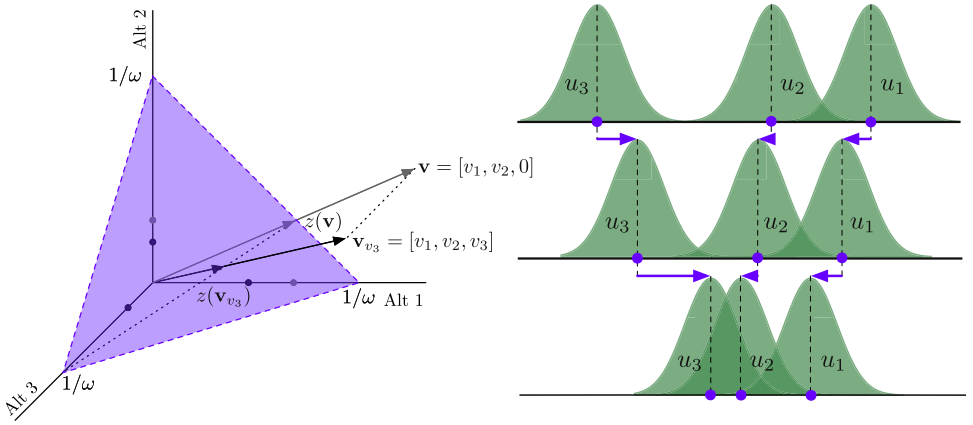

Note. The small circles represent the coordinates of the normalized vector $z(\mathbf{v})$.

error distribution is Gumbel (see also Figure 5 and Appendix B).

Proposition 3 (IIA Violations – Gumbel). *For $v_i > v_j$, a normalized value function $z(\mathbf{v})$, and density function $f(\eta_i) = e^{-(\eta_i + e^{-\eta_i})}$, the introduction of a third alternative v yields relative choice probabilities $\frac{P_i(z(\mathbf{v}_v))}{P_j(z(\mathbf{v}_v))}$, which decreases in v.*

Proof. Consider two values of a third alternative, $v' > v$. Because $v_i > v_j$, then $\frac{P_i(z(\mathbf{v}_v))}{P_j(z(\mathbf{v}_v))} = e^{z_i(\mathbf{v}_v) - z_j(\mathbf{v}_v)} = e^{|z_i(\mathbf{v}_v) - z_j(\mathbf{v}_v)|} < e^{|z_i(\mathbf{v}_{v'}) - z_j(\mathbf{v}_{v'})|} = \frac{P_i(z(\mathbf{v}_{v'}))}{P_j(z(\mathbf{v}_{v'}))}$, for all i, j and all $v' > v$. □

The patterns of IIA violations predicted by normalization depend on the distributional assumption we place on the stochastic term. If we instead assume an independent normal distribution for $\boldsymbol{\eta}$, the pattern of IIA violations predicted by normalization takes a different form (Figure 5). As the value of a third alternative increases, the ratio $\frac{P_1}{P_2}$ still declines, but only until the third alternative starts capturing significant choice probability. Then the ratio $\frac{P_1}{P_2}$ increases and the first alternative is chosen relatively more often. Given the absence of a closed form for the normal distribution, a formal statement along the lines of Proposition 3 is not possible; however, intuition for this result can be found in Figure 4. As the density of u_3 shifts to the right, it overlaps substantially with the density of u_2 before that of u_1. This sends the probability of choosing the second alternative quickly to zero and results in a substitution pattern between alternatives that has a characteristic "u-shape" (Figure 5).

These behavioural predictions of Divisive Normalization naturally extend to larger choice sets. In a random utility model, adding new alternatives to the choice set will necessarily decrease the probability of choosing an existing alternative. This is because a new alternative has a positive probability of being chosen, no matter how small its value. However, in a model with normalization, there is a second effect to consider. Increasing the number of choice alternatives changes the total value of the choice set thus requires neural activity to be reproportioned (Figure 4). This scaling further depresses the probability of choosing the highest valued alternative and imposes a particular pattern on the choice probabilities of other alternatives. In Section 4.2, we present a new behavioural experiment designed to test for the presence of normalization as the choice set grows and to assess the ability of the normalization model to predict across experiments and subject samples.

3.2. Alternative Models of IIA Violations

Given the predicted substitution patterns of Divisive Normalization, it is important to consider the predictions of alternative models and how we might distinguish between them. For instance, adaptations of the random utility model have been previously proposed in order to relax the IIA axiom, all working through the specification of the error distribution. Importantly, many of these alternative approaches are nested in our specification.

Luce Models. If $\omega = 0$ and $f()$ is the density of the independent Gumbel distribution, Equation (6) reduces to the MNL model with variance proportional to σ^2. This model imposes IIA on the data. If we maintain the Gumbel density but allow $\omega \geq 0$, the Equation (6) belongs to the class of "set-dependent Luce models" (Marley et al. 2008), which relaxes IIA but requires that relative log-odds ratios are still proportionate across choice sets (Appendix B).

Figure 5. Simulated Choice Probabilities From a Discrete Choice Model With and Without Normalization, as v_3 is Varied

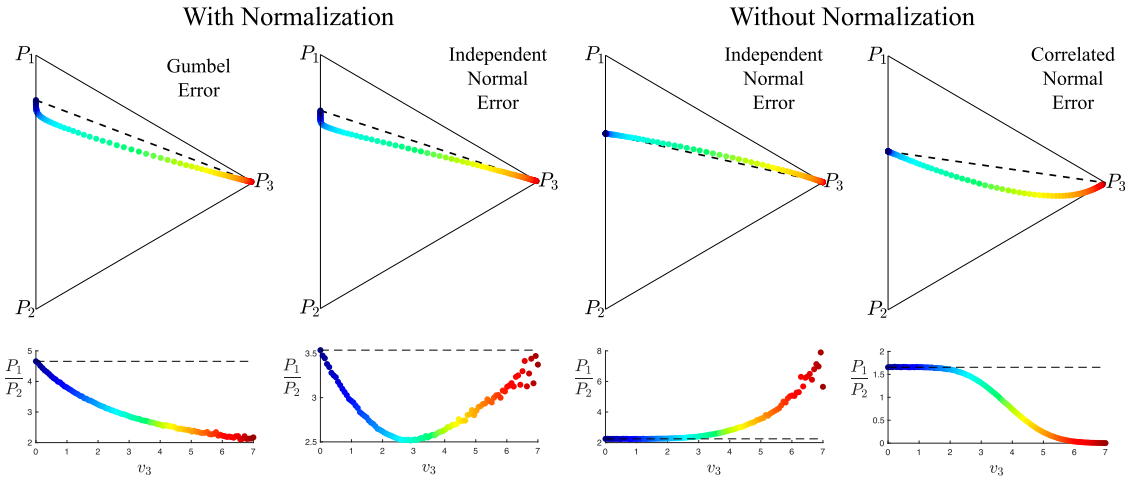

Notes. (Top) T probability simplex; (bottom) the $\frac{P_1}{P_2}$ ratio as a function of v_3. The color in the top figure corresponds to the v_3 in the bottom figure. The IIA property is denoted by the dashed line.

Multinomial Probit. If $\omega = 0$ and $f()$ is the multivariate normal density with a fully parameterized covariance matrix, Equation (6) is the multinomial Probit model. While this specification is flexible, substitution patterns that arise from a relationship between the variances of η_i and the magnitude of valuations in the choice set cannot be captured. Because the lack of a closed-form expression prohibits a definitive statement of which substitution patterns the MNP can and cannot capture, the ultimate test of its limits will have to be empirical.

Range Normalization. We also consider another class of models that normalize valuations by the range of alternatives (Padoa-Schioppa 2009, Soltani et al. 2012, Bushong et al. 2019). A Range Normalization model can implement a bounded value function, provided that the range of valuations is determined by all possible alternatives the decision-maker might encounter. Let $\mathcal{V}$ be this "global" set of valuations (so $\mathbf{v} \subseteq \mathcal{V}$), and denote $\Delta\mathcal{V} \equiv \max \mathcal{V} - \min \mathcal{V}$ as the range of this set. The global range normalization function is then $z_i(\mathbf{v}) \propto \frac{v_i}{\Delta\mathcal{V}}$, by which every possible alternative is normalized on a line between $\frac{\min[\mathcal{V}]}{\Delta\mathcal{V}}$ and $\frac{\max[\mathcal{V}]}{\Delta\mathcal{V}}$. However, this form of range normalization has a substantial empirical drawback. While its value function is bounded, it cannot distort valuations when alternatives are varied within a choice set because $\Delta\mathcal{V}$ remains fixed over choice sets; when an alternative v_3 is added to the set, the normalized valuations $z_1(\mathbf{v})$ and $z_2(\mathbf{v})$ do not change.

For a Range Normalization model to generate substitution patterns, the range of the current choice set must be used. If we let $\Delta\mathbf{v} \equiv \max \mathbf{v} - \min \mathbf{v}$, then a "local" range normalization function is $z_i(\mathbf{v}) \propto \frac{v_i}{\Delta\mathbf{v}}$.[12] This function, however, is not bounded. To see why, consider a binary choice set in which v_1 and v_2 are close together. As the range between v_1 and v_2 shrinks, the normalized valuations $z_i(\mathbf{v}) \to \infty$. Unboundedness is obviously an unappealing property of a model attempting to incorporate constraints on the range of neural activity. Nevertheless, we might still consider the predictions of this unbounded model as the composition of the choice set is varied. In particular, as v_3 grows, the range $\Delta\mathbf{v}$ will shrink, magnifying the difference between z_1 and z_2. In a probabilistic model, this will increase the probability that the highest-valued alternative is chosen. Note that this is the opposite prediction of the value normalization model in Section 3.1.[13]

There is one additional observation to make about the relationship between a normalization model and existing models in the literature. If normalization influences choice behaviour, the model estimates of MNP (or any model without normalization) will be inconsistent. For intuition, it is helpful to consider normalization as a form of heteroskedasticity in the discrete choice model (6), in which the variance is modulated by the elements of the choice set. In contrast to linear models, heteroskedasticity in nonlinear discrete choice models yields both inefficient and inconsistent estimates (Greene 2003). Therefore, if there is indeed normalization present in these data sets, interpreting the estimates from models that explicitly rule out normalization will be problematic. This provides further justification for including normalization in the model specification.

4. Choice Experiments

We now turn to the empirical evidence for how valuations are normalized by the choice set. To test such predictions in a behavioural setting, Louie et al. (2013) developed a two-stage valuation and choice task over common snack food items. The first stage of the experiment elicited a willingness-to-pay (bid) for each item using an incentive-compatible auction mechanism (Becker et al. 1964), which we denote $\mathbf{b} = [b_1, \ldots, b_N]$. This yielded a measure of value for each item in the experiment that is taken *independently* of the other items. In the second stage, subjects then chose a single alternative from choice sets comprised of subsets of these items. Divisive normalization describes how valuations are transformed by the choice set and thus predicts substitution patterns between alternatives when the value and composition of a choice set is varied.

To assess and compare the substitution patterns predicted by Divisive Normalization, Range Normalization, and other competing models, we analyze both the original data set from Louie et al. (2013) for trinary choice sets and present data from a new experiment that varies the size of the choice set. In both data sets, we aim to test the model using purely behavioural measures; therefore, the incentive compatible bids $\mathbf{b}$ are used as an independent measurement of $\mathbf{v}$. Recall that our aim is to assess how valuations, at the time of choice, are transformed by the context of a choice set via the normalization function $z(\cdot)$. Variation in the independent measures ($\mathbf{b}$) across choice sets will allow us to examine the substitution patterns that emerge in choice probabilities via $z(\mathbf{b})$, both nonparametrically and with a structural estimation of the Divisive Normalization model.

A structural analysis is particularly useful because it allows us to compare the Divisive Normalization model to its competitors across experimental designs. One of the benefits of a structural model is that parameter estimates from one data set can be used to predict behaviour in another data set. If the distribution of subject-level parameters is stable across different samples, and if the model is indeed an accurate reflection of behaviour, then the normalization parameters from one data set should provide a good prediction of behaviour in another data set.

All analyses reported in this section are novel, unless specifically noted.

4.1. Trinary Choice Experiment

In the original experiment conducted by Louie et al. (2013), 40 healthy volunteers (21 female, mean age 23.0 years) with normal or corrected-to-normal vision participated in the experiment after giving informed consent. Subjects were instructed to fast for 4 hours before the experimental session and informed that they would have to remain for 1 hour after the completion of the session, during which they could consume only the food item(s) received from the experiment.

In the first stage of the experiment, each subject performed 60 bid trials to establish subject-specific valuations for the array of experimental goods. In each bid trial, subjects viewed a picture of a single snack food item and reported their willingness to pay for that item using a mouse-controlled slider bar ($0–$4 in $0.01 increments). The stimuli consisted of 30 different snack foods presented as high-resolution color images (110 pixels per inch) on a black background; the full list of snack foods and two example images are presented in Appendix D. Other than the visual image, no other information about the snack food was provided to the subject. Items were presented in randomized order, and each individual item was presented twice.

To implement incentive compatibility, each subject was endowed with $4, and if a bid trial was chosen for realization at the end of the session, the outcome was determined via an auction mechanism (Becker et al. 1964).[14] Each of 30 items was shown twice in a randomized order, and multiple bids for the same item were highly correlated ($\rho = 0.9105$, $p < 0.001$, Figure 6). For each subject, each item was then ranked according to its mean bid (Figure 6, Right).

In the second stage of the experiment, subjects chose single items from 250 unique choice sets composed of three alternatives. Choice trials were presented without a time limit and subjects were free to select an item as soon as the choice set was displayed; mean trial length was 2.4 sec, and each trial was followed by an intertrial interval consisting of a blank screen for 1–1.5 sec. At the end of the experiment, one of these choice sets was implemented. Each trinary choice set randomly sampled two alternatives from the 10 highest-valued items (termed alternatives 1 and 2 according to their rank order), and one alternative sampled uniformly from the 20 lowest-valued items (termed alternative 3). Each presented triplet was sampled without replacement and the location of each item on the screen (left, middle, or right) was randomly assigned in each trial. Importantly, this process creates substantial variation in the alternatives labelled 1, 2, and 3 on each trial. In fact, on different trials the same item can be labelled a 1 or a 2, depending on the value of the other alternatives. This provides a strict test of the normalization model because it is highly unlikely that other properties of the individual items are driving the results.

For each alternative in the choice set, the mean of the two bids is denoted b_i, where i is the rank order of that item in a particular set. To facilitate comparison across subjects in the reduced-form analysis, we also report the bid for each item *relative* to the mean bid for all items (within a subject) as the variable $\tilde{b}_i$. Figure 7 reports the choice probabilities across the deciles of all bids, as well as a linear fit over all bids. As might be expected, the choice probabilities increase in the magnitude of the bids.[15]

4.1.1. Reduced-Form Analysis.

We begin our analysis with a comparison of the observed choice frequencies across subjects. Because of heterogeneity in preferences, each subject's bid distribution for the 30 items

Figure 6. (Color online) Bids, Correlation Coefficient, and Ranked Bids

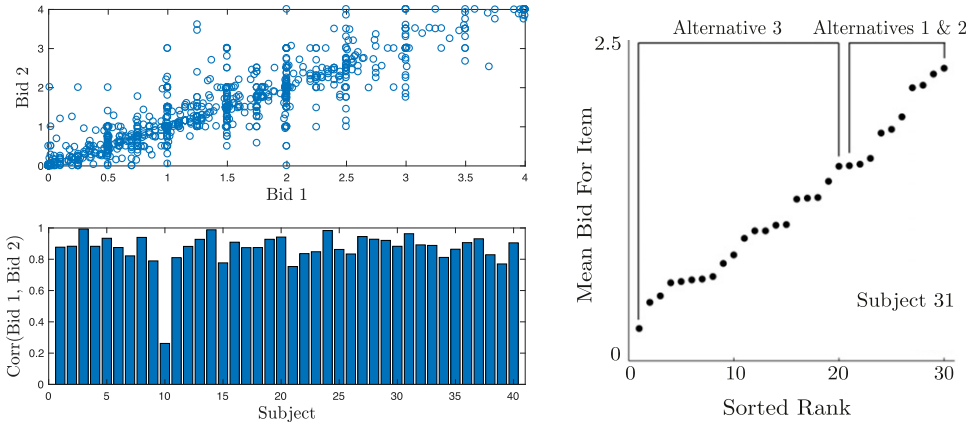

Notes. (Top left) The bids for each item and subject. (Bottom left) The correlation coefficient for each subject. (Right) Ranked bids from an example subject.

Figure 7. (Color online) Sample Choice Probabilities of Each Alternative at the Deciles of All Bids

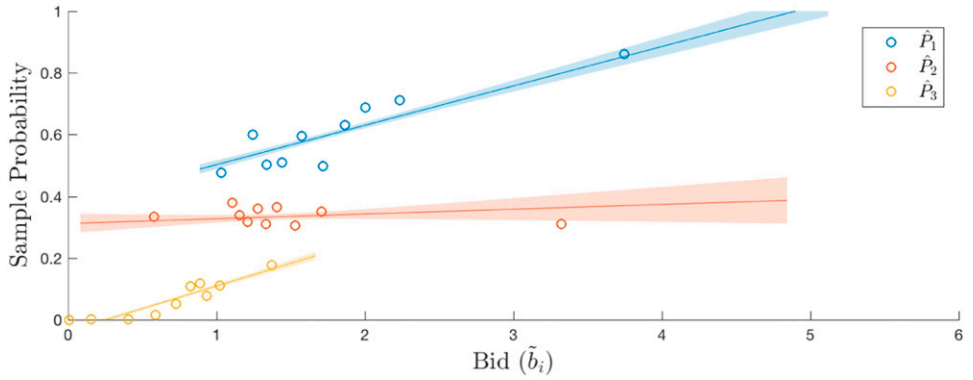

Note. A linear fit over all bids is also depicted.

varied widely. For some subjects, bids for the items that comprise alternative 3 can be close to those for alternatives 1 and 2, whereas for other subjects, they can be substantially lower. This across-subject variation provides our first test. Under normalization, we should expect to see lower odds of choosing alternative 1 versus 2 for subjects with higher bids for alternative 3.

This is indeed the case. Figure 8 reports the subject-level sample probabilities $\hat{P}_1$, $\hat{P}_2$, $\hat{P}_3$ across all choice sets, ordered by the average $\tilde{b}_3$ of each subject. A linear regression on the probabilities for each alternative is also depicted. Not only does the choice ratio between alternatives 1 and 2 decrease, but the probability that alternative 2 is chosen ($\hat{P}_2$) increases by ~ 0.19 as the average $\tilde{b}_3$ increases ($p < 0.043$, two-tailed).[16] Across the sample, the ratio in which subjects select the highest and second-highest alternative decreases by a factor of 2.5 when the value of the third-highest alternative is increased. Subjects who tended to have higher valued third-ranked items chose their highest-ranked items nearly 20% less frequently, and chose their second highest-ranked item nearly 15% more often.

Whereas an across-subject result is suggestive, the critical prediction is normalization at the trial level, depending on each subject's evaluation of the choice set encountered. For instance, note that the above pattern could arise if, by chance, subjects in our sample with a larger average $\tilde{b}_3$ also tend to have smaller value differences between the top two alternatives ($\tilde{b}_1 - \tilde{b}_2$). The Divisive Normalization model introduced in Section 3 controls for this issue by allowing the choice set on a given trial to determine the relative choice probabilities. Before we address the performance of this model, however, it is useful to consider an analysis introduced by Louie et al. (2013), which coded the bid of alternative 3 relative to the mean value of alternatives 1 and 2 on each trial ($b_3 - \frac{b_1+b_2}{2}$). This metric alleviates issues with differing bid ranges across subjects by focusing solely on the composition of the set on each trial. The analysis then dropped the trials in which alternative 3 was chosen, and a logit choice model was fit to the remaining data segregated into five bins of ($b_3 - \frac{b_1+b_2}{2}$). Relative preference is therefore inferred from a binary choice between the alternatives 1 and 2 (within a bin of alternative 3), controlling for differences in valuations of the top two alternatives. The magnitude of a logit parameter (the "steepness" of the logistic function)

Figure 8. (Color online) Sample Choice Probabilities of Each Alternative Plotted Across Subjects by the Average $\tilde{b}_3$ for Each Subject

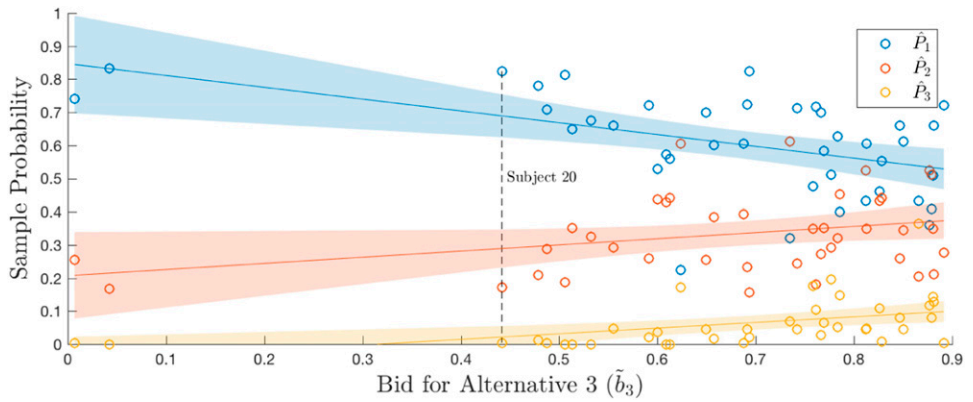

Note. Subject 20 is depicted as an example.

therefore gives a measure of the ratio $\frac{P_1}{P_2}$ at the mean value for $b_1 - b_2$. Essentially, this method assumes that IIA holds "locally" within a bin in order to assess whether it is violated "globally" over bins.

Figure 9 reports two measures of the probability ratio $\frac{P_1}{P_2}$. The first is the ratio of the raw sample probabilities over the top two alternatives $\frac{\hat{P}_1}{\hat{P}_2}$, binned over the quintiles of the bids for the third alternative in the set. The second is the main result reported by Louie et al. (2013). In both analyses, the relative probability of choosing the highest ranked item significantly decreases as the value of alternative 3 approaches the top two alternatives. There is also evidence for a "u-shape" in relative choice probabilities; the probability ratio between alternatives 1 and 2 rises as the third alternative reaches the average for the top two. This substitution pattern is consistent with a normalization model with a normal distribution for $\boldsymbol{\eta}$, as described in Section 3.1. We will now examine the form of this normalization, whether existing models can also capture it, and whether it is robust across experimental paradigms.

4.1.2. Estimation Results and Model Comparison — Pooled. We now turn to estimation of the Divisive Normalization model introduced in Section 3 and a comparison with three alternative specifications: the Multinomial Logit (MNL), Multinomial Probit (MNP), and Range Normalization model defined in Section 3.2. To compare these models, we restate Equation (6) in terms of the observed bids.

$$P_i(\mathbf{b}) = \int \mathbb{1}\left[\frac{b_i - b_j}{\sigma + \omega\left(\sum_n b_n^{\beta}\right)^{\frac{1}{\beta}}} > \eta_j - \eta_i, \quad \forall j \neq i\right] f(\boldsymbol{\eta})\, \mathrm{d}\boldsymbol{\eta}. \tag{7}$$

This specification Equation (7) has an important property; the parameter ω measures the influence of the choice set composition on overall variance. Because a null hypothesis of $\omega = 0$ nests the MNP and MNL, it therefore yields a nested log-likelihood ratio test for the presence of normalization in a data set. We begin with a pooled analysis on the full data set (250 trials × 40 subjects = 10,000 observations) and describe each of these models in turn.

Divisive Normalization. We estimate three different specifications allowing the variance in the model to be determined by the value of alternatives in the choice set (i.e., $\omega \geq 0$):

- To verify that substitution patterns in the data set can be captured solely by Divisive Normalization, we restrict $\beta = 1$ and the covariance matrix of $\boldsymbol{\eta}$ to be independent normal (parameterized by its Cholesky decomposition: $l_{2,2} = 0.866$, $l_{2,1} = 0.5$).[17] In this specification, σ represents the constant portion of the variance and the term governed by ω represents the normalized portion of the variance. This is the original model proposed by Louie et al. (2013).
- To determine the form of Divisive Normalization and how it compares to the MNP, we relax the restriction on β for a total of three parameters (σ, ω, β). This specification has the same number of parameters as the MNP.
- Finally, we estimate a full specification that nests both Divisive Normalization and the MNP. This specification unrestricts the covariance matrix for $\boldsymbol{\eta}$ parameterized by $l_{2,1}, l_{2,2}$ for a total of five parameters $(\sigma, \omega, \beta, l_{2,1}, l_{2,2})$.

In each of these specifications, if we find our estimate of ω to be significantly positive, we can reject a model with constant variance in favour of a model with normalization.[18] Model estimates are reported in columns 4–6 of Table 1. In each of the Divisive Normalization specifications, we find our estimate of ω is significantly greater than zero ($p < 0.001$, LR test).

Figure 9. (Color online) Ratio of the Sample Probabilities and Coefficient From the Logistic Fit of Choice

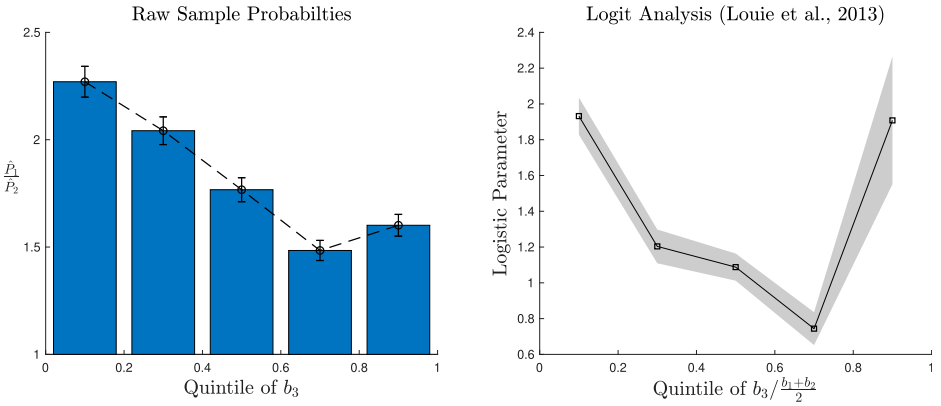

Notes. (Left) Ratio of the sample probabilities for the top two alternatives, binned over the quintiles of the third alternative. (Right) Coefficient from a logistic fit of choice between the top two alternatives, over the range of the third alternative in the set (normalized on each trial), reported by Louie et al. (2013).

Table 1. Estimates of the Divisive Normalization Model and Alternative Specifications for the Trinary Choice Experiment

				Divisive normalization						
	MNL	Probit	MNP	Symmetric recurrent weights			Asymmetric weights		Range normalization	
$\hat{\sigma}$	0.880 (0.036)	0.996 (0.004)	1.493 (0.053)	0.114 (0.024)	0.012 (0.022)	0.121 (0.049)	0.056 (0.026)	0.027 (0.025)	0.439 (0.028)	0.977 (0.100)
$\hat{\omega}$	0	0	0	0.177 (0.007)	0.412 (0.014)	0.183 (0.051)	0.032 (0.007)	0.214 (0.045)	0.370 (0.023)	0.252 (0.050)
$\hat{\omega}_i$	—	—	—	—	—	—	0.177 (0.003)	0.303 (0.048)	—	—
$\hat{\beta}$	1	1	1	1	25.74	0.723 (0.135)	1	3.458 (0.865)	—	—
$\hat{l}_{2,2}$	—	0.866	0.792 (0.033)	0.866	0.866	0.780 (0.044)	0.866	0.866	0.866	0.749 (0.044)
$\hat{l}_{2,1}$	—	0.5	0.431 (0.022)	0.5	0.5	0.454 (0.029)	0.5	0.5	0.5	0.513 (0.030)
LL	–8190.54	–8153.55	–7969.81	–7944.39	–7881.25	–7803.86	–7874.29	–7865.20	–8035.61	–7955.42
BIC	16390	16316	15967	15907	15790	15654	15776	15767	16089	15948
LRT of $\hat{\omega} = 0$ (p-value)				0.000	0.000	0.000	0.000	0.000	0.000	0.000
i. Posterior model prob.		0.000		1.000					0.000	
ii. Posterior model prob.		0.000			0.000			1.000	0.000	
iii. Posterior model prob.			0.000			1.000				0.000
iv. Posterior model prob.	0.000	0.000	0.000	0.000	0.000	1.000	0.000	0.000	0.000	0.000

Notes. Results are pooled over subjects. The reported posterior model probabilities are for (i) models that simply allow normalization versus not ($\omega = 0$ or $\omega \geq 0$), (ii) models that allow different forms of normalization (e.g., $\beta > 0$, $\omega_i \neq \omega$), (iii) models that unrestrict the covariance matrix of $\boldsymbol{\eta}$, and (iv) all models considered. Standard errors are in parentheses. Restricted parameters are in red. A dash represents parameters not present in the specification.

This suggests that the composition of the choice set affects the degree of variance in choice behaviour — and therefore the relative probabilities — in a manner consistent with the normalization model presented in Section 3.[19]

Multinomial Probit. To determine whether the MNP can capture the substitution patterns we observe in this data set, we also estimated the MNP model ($\omega = 0, \beta = 1$) with an unrestricted covariance matrix for a total of three parameters ($\sigma, l_{2,1}$, and $l_{2,2}$), reported in column 3 of Table 1. The log-likelihood of the MNP was lower than each of our restricted normalization specifications, the BIC was higher, and a nonnested likelihood ratio test (Vuong 1989) rejects the MNP in favour of the three-parameter normalization specification with an independent covariance matrix ($p < 0.001$). Not surprisingly, the worst performing specification was the MNL because it imposes IIA.

Range Normalization. To estimate the Range Normalization model, we replace the divisive normalization term in the denominator of Equation (7) with its counterpart for range normalization that is "local" to the choice set: $\sigma + \omega(\max \mathbf{b} - \min \mathbf{b})$. The baseline specification of this model has two free parameters, σ and ω, which again govern the constant and normalized portion of the variance, respectively. We also estimate a full specification with an unrestricted covariance matrix for a total of four parameters. The Divisive Normalization specification outperforms both specifications of the Range Normalization model in terms of a larger log-likelihood and a smaller BIC (columns 9 and 10 of Table 1).

To gauge why the divisive normalization model yields this improvement in fit, we analyzed the predicted probabilities from each of these models using the reduced-form analysis from Louie et al. (2013). Given the estimates in Table 1 and the bids for each subject, we simulated choice data from each of the models and conducted the logistic analysis described in Section 4.1.1. The results are reported in Figure 10. Only the Divisive Normalization model is able to capture the u-shaped choice probability ratio observed in the data, with the minimum of this ratio determined by the magnitude of β. In contrast, both the MNP and the Range Normalization model predict that this ratio should increase as the bids for the third alternative increases.

Finally, we used the estimated BIC for each model to approximate the posterior model probabilities across

Figure 10. (Color online) Logistic Analysis From Louie et al. (2013)

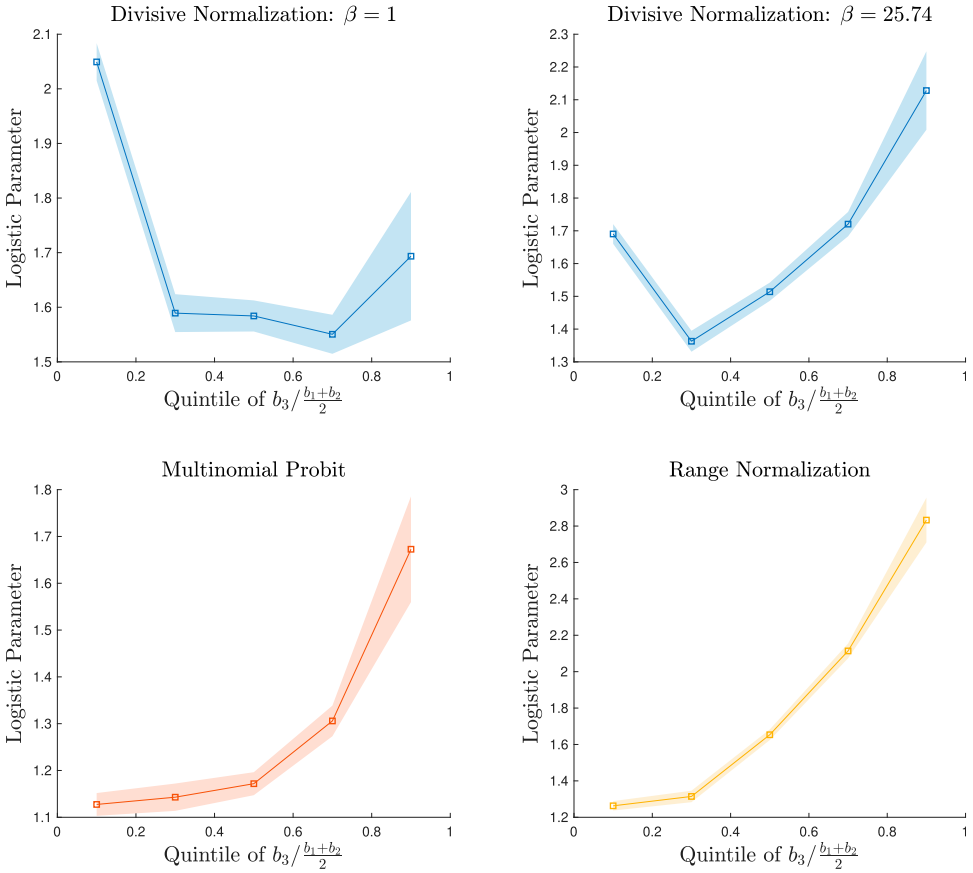

Note. Logistic analysis repeated on simulated data given the parameterizations estimated in Table 1.

subsets of models (e.g., Wasserman 2000, Hawkins et al. 2015). We considered three subsets: models that simply allow normalization versus not ($\omega = 0$ or $\omega \geq 0$), models that allow variation in the form of normalization (e.g., $\beta > 0$, $\omega_i \neq \omega$), and models that unrestrict the covariance matrix of $\boldsymbol{\eta}$. We also calculated posterior model probability across all models considered. Given the substantially smaller BIC for the Divisive Normalization model(s) compared with Range Normalization and the MNP, each of these analyses places a posterior model probability near one on a Divisive Normalization model.

4.1.3. Asymmetric Weights in Normalization. The sensory neuroscience literature suggests that the divisive normalization computation might weight self-inhibitory connections more strongly than the connections across stimuli (Carandini et al. 1997, Rust et al. 2006). If this is also the case for the normalization of valuations, relaxing the restriction that all weights are identical will result in a better fitting model. Therefore, we also considered a Divisive Normalization specification that allows ω_i, the self-referring weight for alternative i, to differ from the weights for all other alternatives. The estimated specification is given by Equation (7) with the normalization function replaced by

$$z_i(\mathbf{b}) = \frac{b_i}{\sigma + \left(\sum_{n \neq i} \omega b_n^{\beta} + \omega_i b_i^{\beta}\right)^{\frac{1}{\beta}}}. \tag{8}$$

A model that unrestricts the normalization weights may also provide a better estimate of β. If the self-referring weight ω_i is larger than for the "cross" weights, ω, then the denominator for the first alternative will largely be driven by this maximal value. However, a model that artificially restricts these weights might then yield an estimate for β, which is too large. Recall that when $\omega = \omega_i$, as β grows large the β-norm approaches a max operator thus closely approximates the normalization equation $z_i(\mathbf{b}) \propto \frac{b_i}{\max[\mathbf{b}]}$ (see Section 3.2).

Indeed, this is what we observe in the estimation results (columns 7 and 8 in Table 1). When the weights are restricted to be identical ($\omega_i = \omega$), the estimate of β is significantly larger than 1 ($p < 0.001$, LR test); therefore, the variance in this specification is driven primarily by the highest valued alternative.[20] Although a large value for β is not implausible (recall that it simply reflects the form of the bound constraint

on neural activity and need not be "computed" in any formal sense), we should note that the point estimate of β becomes quite imprecise when it is large. This is because a given change in a large β yields little change in the choice probabilities for a typical choice set in our experiment, thus little change in the log-likelihood.[21]

However, when the restriction on the weights is relaxed, the denominator for each alternative is allowed to vary. We find that $\hat{\omega}_i$ is significantly larger than $\hat{\omega}$ and our estimate $\hat{\beta} = 3.458$ now lies within the range typically observed in sensory systems (a LR test of $\beta = 1$ is rejected, $p < 0.001$). The log-likelihoods of these specifications are also larger than the other specifications, save for the full normalization specification with an unrestricted covariance matrix.

To summarize our results so far, we find the normalization model outperforms both a standard MNP model and a Range Normalization model in the pooled data set. Our estimates of ω suggest that normalization is driving the variance of the choice model (therefore the resulting choice probabilities) and that the weight on the recurrent alternative ω_i is larger still. Our estimates on the form of the normalization constraint suggest that β lies within the realm typically observed in sensory systems, but estimates become less precise as β increases.

4.1.4. Estimation Results and Model Comparison — Modelling Heterogeneity. To assess how well the Divisive Normalization can model the behaviour of a random participant in our sample, we also consider a random-coefficients specification for the normalization term in Equation (7).[22] Specifically, we let the normalization parameter for each subject ω_s be drawn from the Gamma density $g(\omega_s; a, d)$ with shape parameter a and scale d. The probability of observing the sequence $\{i_1, \ldots, i_T\}$ of $T = 250$ choices for each subject s is then

$$\int \prod_{t=1}^{T} P_{i_t}(\boldsymbol{b}|\omega_s) g(\omega_s; a, d)\, d\omega_s. \tag{9}$$

The likelihood of observing each sequence for each subject in the sample can then be maximized using standard simulation techniques (Train 2009). Results from this analysis are reported in Table 2 and the estimated density of ω_s for both Divisive Normalization and Range Normalization models are depicted in Figure 11.

The use of the Gamma distribution is particularly informative because it can place substantial density on $\omega = 0$ if the shape parameter a is small. For the Divisive Normalization model, we find that that the estimated density of ω_s places substantial weight on $\omega_s > 0$ for both specifications considered (when $\beta = 1$ and β is unrestricted). The estimate of β is again within the range typically observed in sensory systems. By contrast, the estimated density for the Range Normalization model places much more weight on $\omega_s = 0$ (Figure 11). A random-effect Probit specification was also examined to provide a baseline account of subject heterogeneity (estimates not depicted, $LL = -7562.61$, BIC = 15,143). Both Divisive Normalization specifications have a larger log-likelihood and a smaller BIC compared with the Probit with a random effect, while Range Normalization performs the worst. A combined model with random effects for both ω and σ provides a significantly better fit than a model with only a random effect for σ (LRT = 66.54, $p < 0.000$). All together, these results suggest that Divisive Normalization captures an important component of the variance in this data set.

Table 2. Random Coefficient Model Estimates for the Trinary Choice Experiment

	Divisive normalization		Range normalization
$\hat{a}$	1.823 (0.355)	2.115 (0.422)	0.523 (0.143)
$\hat{d}$	0.108 (0.025)	0.1569 (0.050)	0.945 (0.306)
$\hat{\sigma}$	0.069 (0.027)	0.049 (0.327)	0.397 (0.021)
$\hat{\beta}$	1	2.208 (1.359)	—
LL	−7541.95	−7538.88	−7620.70
BIC	15112	15115	15269
Posterior model prob.	0.823	0.177	0.000

Notes. Standard errors are in parentheses. Restricted parameters are denoted in red.

4.2. Set Size Experiment

The Divisive Normalization model makes additional predictions about how choice probabilities should change as the set size increases. An increase in the number of choice alternatives increases the total value of the choice set, thus reproportions valuations according to the number of items in the set (Figure 4). This depresses the probability of choosing the highest-valued alternative relative to a random utility model. To test for this predicted pattern, we developed a two-stage experimental design that varies the size of the choice set.

This experiment also allows us to examine the robustness of our proposed Divisive Normalization model. One of the benefits of structural estimation is that, in principle, the distributions of structural parameters should be invariant. We can therefore examine how well the parameters from the trinary experiment, estimated via the structural specification (7),

Figure 11. Probability Density of $\omega_s \sim \text{Gamma}(a, d)$ Estimated From the Trinary Experiment

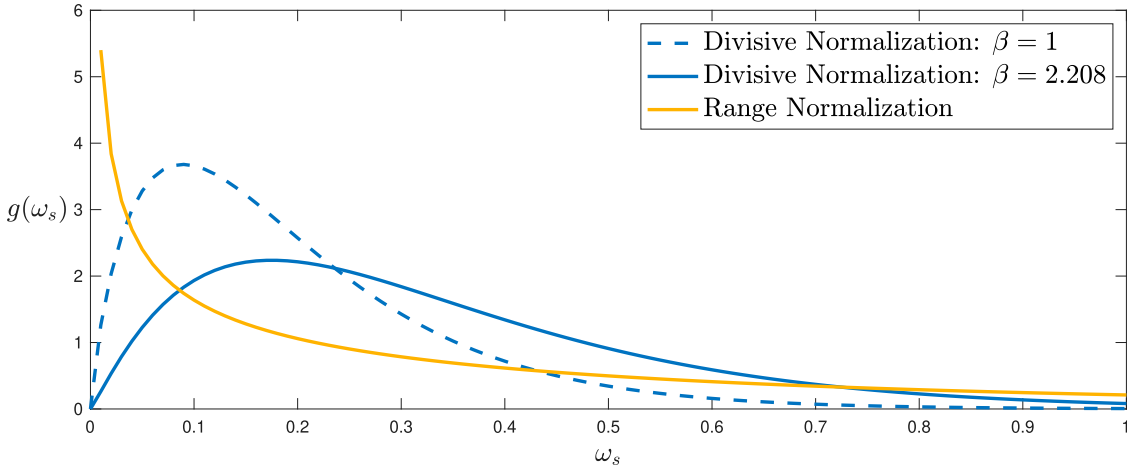

are able to capture the choice behaviour of a new set of subjects performing a different experiment.

4.2.1. The Set Size Task. Our set size task had a similar structure to the trinary choice experiment. In the initial valuation stage, 30 subjects (11 female, mean age 24.4 years) reported their maximum willingness to pay for 30 individual snack food items, twice each (60 trials total). For each subject, items were then ranked according to their mean bid value, and the 10 highest-valued and 10 lowest-valued items were selected for inclusion in the second stage of the experiment.

In the second stage, subjects performed 270 choice trials from choice sets of varying sizes. On each trial t, a choice set consisted of two high-value alternatives (again, denoted alternatives 1 & 2 in rank order) and a variable number of randomly chosen low-valued items for a total set size of $N_t \in \{2, 4, 6, 8, 10, 12\}$ items. Choice sets were constructed to include varying target value differences, with 45 different trials in each set size condition. On a given trial, item images were randomly assigned to one of 12 possible locations on the computer screen. Subjects were free to select an item as soon as the choice set was displayed, and there was

Figure 12. Fitted Probabilities and Out-of-Sample Predicted Probabilities For The Set Size Experiment

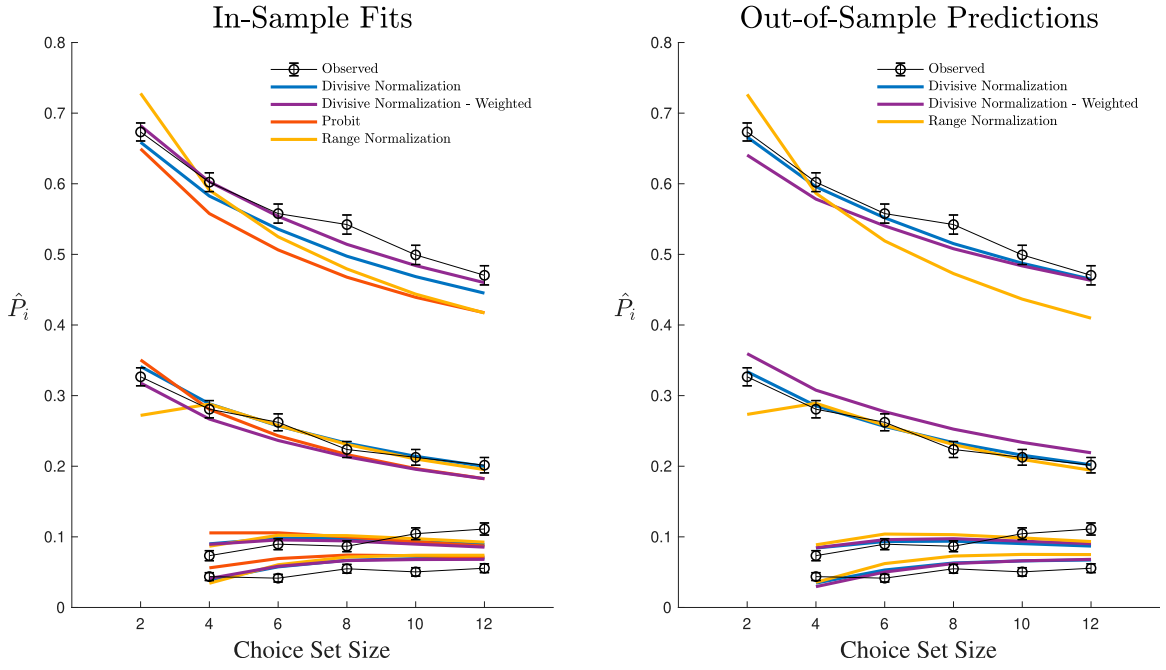

Notes. (Left) The fitted probabilities that alternative 1, 2, 3, and 4 are chosen (from top to bottom), over the range of choice set sizes. (Right) The out-of-sample predicted probabilities using the estimates from the trinary experiment.

Table 3. Maximum Likelihood Estimates for Set Size Experiment

		Divisive Normalization						
	Probit	Symmetric weights		Asymmetric weights		From trinary		Range normalization
$\hat{\sigma}$	1.210	0.985	0.001	0.022	0.000	0.012	0.027	0.441
	(0.016)	(0.042)	(0.009)	(0.011)	(0.008)			(0.034)
$\hat{\omega}$	0	0.020	0.442	0.055	0.492	0.412	0.214	0.357
		(0.004)	(0.075)	(0.003)	(0.010)			(0.019)
$\hat{\omega}_i$				0.205	0.460		0.303	
				(0.056)	(0.020)			
$\hat{\beta}$	1	1	18.85	1	51.88	25.74	3.458	
			(7.715)		(36.69)			
LL	−10066.22	−10049.83	−9723.77	−9957.17	−9695.79	−9739.98	−9972.41	−9914.31
BIC	20142	20118	19475	19942	19428	19480	19944	19847
LRT of $\hat{\omega} = 0$ (p-value)		0.000	0.000	0.000	0.000			0.000
i. Posterior model prob.	0.000		0.992			0.008		
ii. Posterior model prob.	0.000	0.000	0.000	0.000	1.000			0.000

Notes. The reported posterior model probabilities are for (i) a comparison of Divisive Normalization with the model fits from the trinary experiment and (ii) all models fit on the set size data. Standard errors are in parentheses. Restricted parameters are denoted in red, including parameter values taken directly from the trinary experiment in Table 1.

no time limit for making a selection; mean trial length was 3.1 sec, and each trial was followed by an intertrial interval consisting of a blank screen of 1–1.5 sec. The remainder of the experimental design, including payment methods, were identical to the trinary choice experiment.

4.2.2. Estimation Results and Model Comparison — Pooled. As expected, increasing the size of the choice set decreases the probability that the highest ranked alternative is chosen. In our largest set size of 12 alternatives, this probability decreases by 20% (Figure 12). Of course, any random utility model will have this qualitative feature. Therefore, to determine if this decrease is better captured by a choice model with normalization, it is crucial to use a structural specification that controls for the size and valuations of the items in the set. To do so, we estimate the normalization model (6) with the only difference lying in the number of choice elements, N_t, now varying over trials. This yields the choice probabilities on trial t,

$$P_{i,t}(\mathbf{b}) = \int \mathbb{1}\left[\frac{b_{i,t} - b_{j,t}}{\sigma + \left(\omega_i b_{i,t}^{\beta} + \sum_{n \neq i} \omega b_{n,t}^{\beta}\right)^{\frac{1}{\beta}}} > \eta_{j,t} - \eta_{i,t}, \forall j \neq i\right] f(\boldsymbol{\eta}_t) d\boldsymbol{\eta}_t. \tag{10}$$

As in the trinary case, we initially restrict $\omega_i = \omega$ to provide a nested hypothesis test of the standard Probit model. Because the number of alternatives differs over trials, we restrict the covariance matrix of $\boldsymbol{\eta}$ to be independent normal. This also allows a direct comparison with the estimates from the same specification in the trinary experiment reported in Section 4.1.2.

The resulting maximum likelihood estimates for the entire pooled sample are reported in Table 3 for five nested specifications: the Probit, the simple normalization model proposed by Louie et al. (2013), a normalization model with β unrestricted, and two specifications that relax restrictions on ω_i. We also estimate a Range Normalization model as in Section 4.1.2.

In each of our Divisive Normalization specifications, we find that the estimate of ω is significantly different from zero ($p < 0.001$, LR test). This suggests that we are observing choice behaviour in which the

Table 4. Random Coefficient Model Estimates for the Set Size Choice Experiment

	Divisive normalization		Range normalization
$\hat{a}$	0.839	1.400	0.615
	(0.028)	(0.274)	(0.120)
$\hat{d}$	0.166	0.346	1.128
	(0.123)	(0.102)	(0.379)
$\hat{\sigma}$	0.163	0.000	0.283
	(0.040)	(0.024)	(0.018)
$\hat{\beta}$	1	4.349	—
		(0.6971)	
LL	−8971.17	−8759.86	−8933.98
BIC	17951	17528	17877
Posterior model prob.	0.000	1.000	0.000

Notes. Standard errors are in parentheses. Restricted parameters are denoted in red.

composition of the choice set affects the degree of variance in the model and therefore the relative choice probabilities. The best performing model unrestricts both ω_i and β, though the point estimate of β is again large and relatively imprecise. As in the trinary experiment, the unrestricted Divisive Normalization models significantly outperform Range Normalization in terms of log-likelihoods and BIC.

The fitted probabilities over the different choice set sizes are reported in Figure 12. The Divisive Normalization model captures the sample choice probabilities for all set sizes, with the slight exception of underpredicting the probability of choosing alternative 3 in large set sizes.[23] This is in contrast to the Range Normalization and Probit models. While Range Normalization is unable to capture the change in probability of choosing the highest alternative as the set size increases, the Probit underpredicts this probability for all set sizes. As a result, for a set size of 12 alternatives, the highest ranked alternative is chosen 5% more often than predicted by a Range Normalization model and the Probit model with a constant variance.[24]

Finally, we assess the robustness of the Divisive Normalization specification across our two experimental paradigms. Remarkably, the degree of normalization that we observe is largely consistent with the estimates from the same specification of the trinary experiment ($\hat{\sigma}$: 0.001 versus 0.012; $\hat{\omega}$: 0.442 versus 0.412; and $\hat{\beta}$: 18.85 versus 25.74). Restricting the model to the parameter estimates from the trinary experiment yields a slight increase in the log-likelihood (Table 3, second-to-last column), suggesting that the same normalization parameters can capture the relationship between the choice probabilities and the composition of the set across the two experiments. To assess this result, we used the estimated parameters from the trinary experiment to generate predicted choice probabilities for the choice sets in the set size experiment via Equation (10). Figure 12 reports these out-of-sample predicted probabilities. We should emphasize that these are aggregate predictions conducted on a completely separate sample of subjects from a different experimental paradigm. Notably, the Divisive Normalization model captures the sample choice probabilities for all set sizes, with the exception of underpredicting the probability of choosing alternative 3 when the set size becomes very large.

4.2.3. Estimation Results and Model Comparison — Modelling Heterogeneity. To model heterogeneity in the set size sample, we also considered the random-coefficients specification from Section 4.1.4, in which the normalization parameter for each subject ω_s is drawn from the gamma density $g(\omega_s; a, d)$ with shape parameter a and scale d. Results from this analysis are reported in Table 4 and the estimated density of ω_s for both Divisive Normalization and Range Normalization models are depicted in Figure 13.

In the case of the Divisive Normalization model, we find that a is significantly different from zero and that the estimated density of ω_s places substantial weight on $\omega_s > 0$ for the specification with β unrestricted. The estimate of β is larger than in the trinary case (4.4349 versus 2.208), but only marginally significantly so ($p = 0.11$) and still within the range typically observed in sensory systems. The specification that restricts $\beta = 1$; however, is summarily rejected. Similarly, the estimated density for the Range Normalization model places much more weight on $\omega_s = 0$. This model has a smaller log-likelihood and a larger BIC compared with Divisive Normalization with an unrestricted β.

5. Conclusion

In the study of the human brain and behaviour, it has long been recognized that the biology of neural systems is both subject to constraints imposed by finite resources and shaped by the statistical properties of the environment in which we live (Machens et al. 2005, Ganguli and Simoncelli 2014, Wei and Stocker 2017). As a

Figure 13. The Probability Density of $\omega_s \sim \text{Gamma}(a, d)$ estimated from the set size experiment.

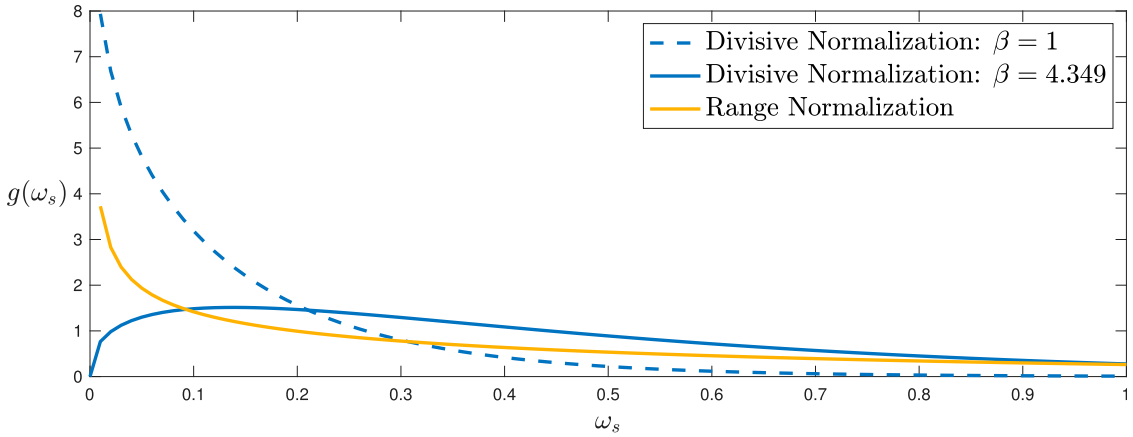

result, it is assumed that the organization and form of neural computations have evolved such that information about the objective world is approximated and/or compressed into quantities that can be encoded in finite, stochastic, neural activity. A growing number of scholars are examining what these constraints imply for choice behaviour and how behavioural theories can incorporate these insights (Caplin and Dean 2015, Steiner and Stewart 2016, Khaw et al. 2017, Bhui and Gershman 2018, Noguchi and Stewart 2018, Frydman and Jin 2019, Polania et al. 2019).

In this article, we study the role of one canonical neural computation, Divisive Normalization, in shaping valuations in response to a bound constraint on neural activity. Because Divisive Normalization suppresses, or normalizes, valuations relative to the composition and size of the choice set, it yields predictions about relative choice probabilities that depend on the choice set. These predictions include increased stochasticity compatible with Weber's law, particular patterns of violation of the Independence of Irrelevant Alternatives axiom, and a decreased likelihood of choosing a higher-valued alternative as the composition of the choice set is altered. In our choice experiments, we find behaviour consistent with these patterns; a choice model with Divisive Normalization outperforms alternative specifications including Range Normalization and the Multinomial Probit. We also document robustness in the estimated model parameters across paradigms. The structural estimates from an experiment that varies the value of a third alternative are very similar to those in an experiment that varies the size of the choice set, even outperforming the alternative models fit in-sample. Such robustness in the estimates of structural preference parameters suggests that Divisive Normalization may be a basic property of choice behaviour.

We also address the normative role of the relative valuations induced by the divisive normalization computation. In sensory systems, normalization has been demonstrated to reduce the costly resources required to encode the statistical properties of our natural environment. However, for decision-making, its predictions are initially puzzling (Louie et al. 2013). In the absence of any constraints, the choice behaviour of subjects in our experiments can be deemed inconsistent or perhaps even welfare-decreasing: for example, the highest-ranked alternative was chosen less when both the composition and the size of the choice set was altered. Why would a neural system – selected over tens of millions of years of evolution – exhibit such adverse choice performance?

We propose that these patterns in choice behaviour are by-products of a boundedly rational decision-making process under neurobiological constraints. Because neural activity is both stochastic and bounded, the normative question must be reframed. How should the brain encode the valuation of choice alternatives given a neurobiological constraint on the precision and resolution with which it can encode quantities and why might this encoding scheme follow the form of Divisive Normalization? Our answer is that some degree of normalization is required to compare choice alternatives. Normalization scales valuations to the boundary of a constraint, preserving relative valuations and yielding the fewest possible choice errors. From the perspective of information coding, Steverson et al. (2019) demonstrate that Divisive Normalization implements a tradeoff between the cost of errors and the cost of reducing stochasticity. Viewed this way, the adverse choice behaviour we observe is not due to an inefficient or mal-adapted neural architecture but is, in fact, an efficient implementation in response to a neurobiological constraint on value representations.

Understanding the mechanism by which the brain encodes relative quantities can be extended into other domains of economic choice behaviour. For instance, choice behaviour in the domain of uncertainty suggests that utilities are determined relative to a reference point (Kahneman and Tversky 1979), perhaps formed as an endogenous expectation over a history Koszegi and Rabin (2006). The Divisive Normalization computation also contains a reference point — in a static environment it is given by the parameter σ. As σ changes, the normalization computation shifts the "domain" over which the range of neural activity encodes stimuli, with the largest change in neural activity located at σ (Louie et al. 2015, figure 3b). A dynamic version of the Divisive Normalization computation explores implications for behaviour when this expectation is formed over time (LoFaro et al. 2014, Zimmermann et al. 2018, Tymula and Glimcher 2019). In particular, Divisive Normalization places greatest discriminability where rewards are most likely (Louie et al. 2015, Frydman and Jin 2019). More generally, these insights have been extended to the multiattribute domain. Landry and Webb (2020) extend the normalization computation to address a range of phenomena including well-known *decoy effects* that rely on a particular structure of numerically presented attributes (Huber et al. 1982, Simonson 1989, Tversky 1972). Related work emphasizes the sequential comparison of attributes relative to a reference sampled from working memory (Noguchi and Stewart 2018).

All together, our results speak to the role of incorporating insights from biology into economic discourse. Although developing an understanding of the brain is intriguing in its own right, the goal of neuroeconomic research should be predicting novel patterns in choice behaviour and producing a normative explanation for the behaviour we observe (Bernheim 2009,

Glimcher 2011). We argue that incorporating divisive normalization into a choice model accomplishes this goal. Our results emphasize both the positive advances offered by choice models grounded in neuroscience, and the normative role neurobiological constraints can play in the study of choice.

Acknowledgments

The authors thank A. Caplin, N.G. Martineau, T. Strzalecki, K. Train, and T. LoFaro for helpful comments, as well as seminar participants at Harvard University, the University of Zurich, Maastricht University, Princeton University, Northwestern University, and the Ohio State University. The authors also thank M. Bukwich, M. Khaw, and R. Daviet for excellent research assistance. This research was funded by the Army Research Office (W911ND-11-1-0482), and the experiments were approved by an ethics review panel at NYU.

Appendix A. The Neurobiology of Sensation, Valuation, and Choice

In this appendix, we review the literature on the neurobiology of choice behaviour. In Appendices A.1 and A.2, we review the neuroscience literature on the Divisive Normalization computation in regions of the brain associated with sensation and valuation. In Appendix A.3 we review the neuroeconomics literature on valuation and choice processes and outline the workhorse "two-stage" model of decision-making.

We begin with some background on the structure of the brain that might be helpful for understanding how decision-making is constrained by neurobiology. The total pool of neurons that make up cortex can be anatomically divided into nonoverlapping subsets of neurons, and each of these "areas" is distinct in structure and organization. Empirical evidence suggests that any given area serves a limited set of functional roles – which are the same across individuals – and a small subset of these areas have been identified as having a role in decision-making. It is essentially required by this logic that devoting more neural resources to these decision-making areas must balance the benefits of improved decision-making against the costs of allocating those resources to other functions, such as processing sensory information or managing the heartbeat.

So why is a decision-maker limited in its ability to recruit more neural resources, even if it might be momentarily advantageous? The reason is that brain areas are distinct in their connections with the rest of the brain, distinct in their cellular structure, and distinct in many of their biophysical properties. These specializations, which distinguish different brain areas and make them appropriate for particular functions, develop over years – primarily over the first 20 years of development – and cannot be altered quickly. This imposes a significant constraint on the ability of a decision-maker to endogenously allocate neural resources to a task. For these reasons, we consider the allocation of neural resources to be effectively fixed at a particular moment in time, at least for the time horizon in which decisions are typically made by an individual.[25]

A.1. Divisive Normalization in Sensory Systems

A fundamental goal in *systems neuroscience* is to understand how the brain processes and represents information at the level of individual neurons. Much of this work has focused on the sensory domain in which an environmental stimulus is transduced through the sensory organs and passes through a series of processing stages (i.e. spatially and functionally distinct networks of neurons), each of which has a particular role. In the visual system, for instance, photons (which comprise light) make initial contact with photoreceptors in the retina and this information passes through subsequent stages of hierarchical neural processing in retinal ganglion cells, the thalamus, primary visual cortex, and so on. Generally speaking, sensory neurons in these regions are "tuned" for a particular stimulus, for instance, the intensity of light in a particular region of visual space, or a particular direction of motion (e.g., Hubel and Wiesel 1968).

At each of these levels, sensory neurons display activity that cannot be solely explained by linear models (the activity of a neuron is not simply a weighted sum of the inputs to that neuron). For instance, neural activity is bounded at high input levels and exhibits the phenomenon of *suppression* — the neural activity elicited by a stimulus (for which the neuron is tuned) is reduced in the presence of a stimulus for which it is not tuned. In the retina, for example, light intensity is encoded relative to the average ambient illumination. This relative representation of information is observed to be a general feature of sensory coding.

The divisive normalization computation was proposed to explain such nonlinear phenomena in primary visual cortex (Heeger 1992). The critical feature of the computation is a divisive rescaling of the activity of a population of neurons by the total activity of a larger pool of neurons. Variations on the form of normalization have appeared in literature, all nested by the general form,

$$f_i(x_1,\ldots,x_N) = \kappa \frac{x_i^{\alpha}}{\sigma + \left(\sum_{n=1}^{N} \omega_n x_n^{\beta}\right)^{\frac{1}{\gamma}}}, \tag{A.1}$$

where the response $f_i(x_1,\ldots,x_N)$ of a population $i \in N$ is a function of both the driving input x_i to that population and the inputs to the other elements of the normalization pool (Lyu and Simoncelli 2008, Lyu 2011, Sinz and Bethge 2013,

Figure A.1. Regions of Visual Space

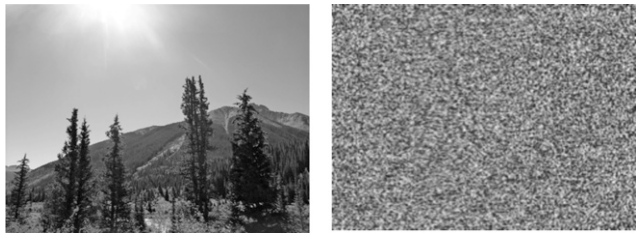

Notes. In the natural environment, nearby regions of visual space tend to be correlated (left), not independent (right). When correlated, information on one region can be used to predict information in a nearby region, therefore it is redundant.

Ballé et al. 2016a). This general response function is governed by a number of parameters: κ denotes the maximum possible activity level, σ determines how responses saturate with increased driving input, ω_n weights each neural population in the normalization pool, and α, β and γ mediate the form of the normalization.

Divisive Normalization implements several features consistent with how neurons in visual cortex respond to sensory information. First, because the input to a given neuron is also included in the normalization pool, the model produces a saturating response to increases in driving input. This is consistent with the observation that neurons are biologically constrained below a maximum firing rate. Second, division expresses the quantity encoded by a population of neurons in relative terms, scaled to the pooled activity of other inputs. Indeed, divisive normalization appears to be a general feature of information processing in cortical systems (for a review, see Carandini and Heeger 2012). Originally proposed to explain nonlinearities in primary visual cortex, normalization has been identified in multiple stages of visual processing from the retina to downstream visual areas, and in species ranging from the fruit fly to primates. In addition to vision, normalization characterizes neural responses in all other sensory modalities, such as audition and olfaction, and extends to higher-order cognitive processes including attention and multi-sensory integration.[26]

Given the pervasive observation of divisive normalization in sensory systems, the question of its normative role in neural coding has been raised. In systems neuroscience, the benchmark normative framework for information processing is the *efficient coding* hypothesis (Barlow 1961) based on Shannon's seminal work on information transmission via finite capacity channels. Because neural systems face biological constraints (e.g., maximum firing rates and/or numbers of neurons), the efficient coding hypothesis holds that sensory stimuli should be represented in a manner that minimizes the redundancy in encoded information; that is, neural responses should be statistically independent. Crucially, the statistics of the natural environment are decidedly not independent (Figure A.1). For instance, regions of visual space with intense light occur in clusters, unlike the statistically independent "snow" displayed on an untuned analog television set. Under the efficient coding hypothesis, sensory systems should transform information about the natural world into a less redundant representation by incorporating these dependencies directly in coding algorithms.

Whereas linear weighting functions can remove some redundancies, the statistics of natural images are too complex for linear models to produce completely independent responses. By contrast, the nonlinear divisive normalization model markedly reduces higher-order correlations in responses to both natural images and sounds (Schwartz and Simoncelli 2001, Lyu 2011, Sinz and Bethge 2013, Ballé et al. 2016a) and has been shown to implement near-optimal categorization and encoding of these sensory stimuli (Qamar et al. 2013, Iyer and Burge 2018). Thus, there is compelling evidence that normalization serves a specific normative role in implementing efficient information coding in sensory systems.

However, this constrained encoding scheme (like all constrained optimal solutions) has consequences. Although the encoding itself is efficient given the constraint, it can still lead to errors in perception, and ultimately, choice. Consider the image known as the "Checkerboard Illusion" depicted in Figure A.2. If required to decide which of the two regions "A" and "B" appears brighter, one could not be faulted for choosing B. In fact, the luminance of the two regions is precisely the same. However, B *appears* brighter due to the normalization computation performed at the level of the retina and visual cortex. The luminance of region B is encoded relative to nearby locations that fall in a shadow and is therefore normalized to a lesser extent than A. Therefore, B appears brighter even though it is of the same (objective) luminance, potentially resulting in a choice error.

A.2. Divisive Normalization of Valuations

The ubiquity of divisive normalization in sensory brain areas, and the general similarity of information processing in neural systems, suggests that a form of normalization may also be taking place in regions of cerebral cortex that are involved in decision-making. Recent neural evidence from frontal and parietal regions of the primate brain supports this contention (Rorie et al. 2010, Louie et al. 2011, Pastor-Bernier and Cisek 2011, Yamada et al. 2018). For example, Louie et al. (2011) examined the activity of neurons

Figure A.2. (Color online) The "Checkerboard Illusion"

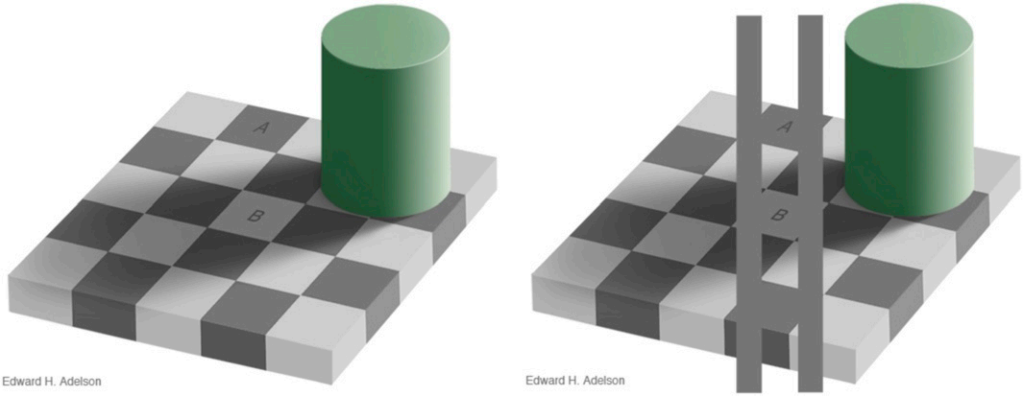

Source. Reproduced with permission from http://persci.mit.edu/gallery.
Note. Regions A and B have equal luminance.

in the LIP area of the monkey brain (Figure A.3). Previous work has demonstrated that the activity of individual LIP neurons varies with the quantity of the reward associated and is involved in the selection of actions (see Appendix A.3.2). In the Louie et al. (2011) experiment, multiple alternatives were displayed on a screen, and the value of one alternative (in 1 mL of water) was held constant while the number and value of the other alternatives were varied. In the absence of normalization, varying the other alternatives should elicit no change in activity from the neuron which encoded for the constant target. Nonetheless, the measured neural activity varied inversely with the number and value of the alternatives, consistent with a model in which the neural activity coding the value of a specific alternative is suppressed by the value of others. Furthermore, a simple Divisive Normalization model provides a stronger account of this neural data than other candidate explanations, suggesting a common form of information coding in sensory and decision-related neural activity. Such relative value coding is likely to be a common feature of action-selective decision areas, empirically demonstrated in parietal cortex (Rorie et al. 2010, Louie et al. 2011), orbito-frontal cortex (Yamada et al. 2018), dorsal premotor cortex (Pastor-Bernier and Cisek 2011), striatum (Wang et al. 2013, Klein et al. 2017), and the superior colliculus (Basso and Wurtz 1997). Reviews of this literature can be found in the works of Seymour and McClure (2008), Rangel and Clithero (2012), and Louie et al. (2015).

A.3. A Two-Stage Model of Valuation and Choice

To examine the role of Divisive Normalization in shaping valuations during choice, we focus on a basic two-stage decision model in the primate brain. This model is predicated on a distinction between brain regions that aggregate value information from attributes in an action-independent manner and those that employ that value information in the process of choice (Platt and Plassmann 2013, Polania et al. 2015). In Figure A.4, we provide a conceptual description of this model. We should emphasize that our focus on the simple two-stage formulation of valuations and choice is to highlight the role normalization plays in shaping valuations as they transition between frontal and parietal regions of the brain during decision-making. This model can be expanded to allow for multiple stages of processing with interaction between these stages (e.g., Cisek 2012, Platt and Plassmann 2013, Cai and Padoa-Schioppa 2014, Hunt and Hayden 2017). Indeed, it has been recently proposed that information transitions through multiple levels of processing with a computation akin to Divisive Normalization at each of these levels (Yoo and Hayden 2018). This flow of

Figure A.3. The Louie et al. (2011) Experiment in Which a Monkey Is Evaluating choice Alternatives

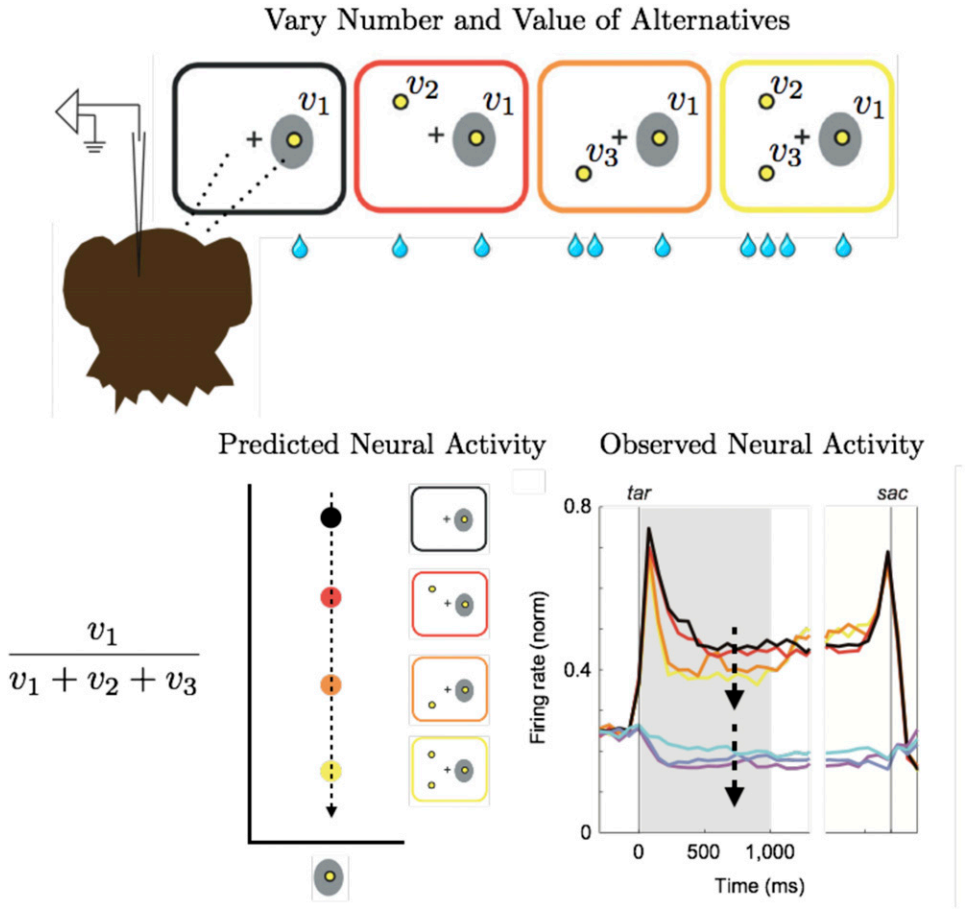

Notes. Neural activity is recorded for a constant alternative v_1 (grey circle), while the number and value (in μl of water) of the other alternatives is varied. The average activity (firing rate) of the recorded neurons over the course of the trial is reported.

information can arise indirectly through other cortical or subcortical structures and therefore does not require direct connectivity between cortical regions (Moisa et al. 2018).

A.3.1. The First Stage: Value Integration The representation of an integrated value signal in frontal brain regions is supported by multiple lines of evidence, including anatomical connectivity, neural activity recordings, and lesion studies. Consistent with a region performing integrative valuation, anatomical studies document that frontal brain regions receive sensory inputs from visual, auditory, gustatory, olfactory, and somatosensory systems along with memory systems in perirhinal cortex and hippocampus (Ongür and Price 2000, Camara et al. 2009, Shadlen and Shohamy 2016).[27] Neurophysiological and neuroimaging studies further support the hypothesis that frontal areas are involved in the integration of value information. Over 200 studies have demonstrated that activity in these brain regions is correlated both with the valuations that humans place on different items, as well as information about the individual attributes from which those values are derived (for reviews, see Bartra et al. 2013, Levy and Glimcher 2012, and Clithero and Rangel 2013).[28]

Consistent with a representation of integrated value (a neural "common currency"), frontal brain regions encode multiple aspects of individual rewards such as magnitude, probability, and sensory features (Tremblay and Schultz 1999, Kennerley and Wallis 2009, Rich and Wallis 2016) and correlate with the willingness to pay of a range of different objects such as food, consumer items, lotteries, and social rewards (Plassmann et al. 2007, Chib et al. 2009, FitzGerald et al. 2009, Lin et al. 2012). Importantly, information about specific attributes or good categories is most distinguishable in lateral and ventral regions of orbito-frontal cortex (Hare et al. 2011a, McNamee et al. 2013, Suzuki et al. 2017), suggesting that attribute-level information is integrated into a neural representation of value as it transitions toward medial prefrontal areas. It is these latter regions that can be used to measure valuations of consumer items in the absence of choice behaviour (Levy and Glimcher 2011, Smith et al. 2014) and have been shown to correlate with the willingness to pay measured from bidding procedures on consumer goods (Plassmann et al. 2007, Chib et al. 2009).[29] In our model, these valuations are denoted $\mathbf{v} = [v_1, \ldots, v_N]$ for the alternatives $\{1, \ldots, N\}$ and are measured directly using a willingness-to-pay procedure.

A.3.2. The Second Stage: Action Selection In the second stage of neurobiological decision-making, subjective (or constructed) value information is utilized by neural circuits that implement a decision. The predominant model for this choice process is based on models of perceptual decision-making (Gold and Shadlen 2007, Cisek and Kalaska 2010, Summerfield and Tsetsos 2012, Shadlen and Kiani 2013), in which decisions are physically implemented as arm reaches or eye movements, and neural activity is examined in the relevant brain structures.[30] These brain structures typically receive both bottom-up sensory information and top-down information from frontal brain regions, perhaps indirectly through cortical and subcortical structures like striatum (Polania et al. 2015, Moisa et al. 2018) and are closely related to movement-related circuits.[31] Critically, activity in these brain regions also covary with the values of the rewards associated with those particular actions, suggesting that this *action value* information is incorporated into the dynamic processes that determine choice. However, in contrast to first-stage brain regions, neural activity in second-stage areas represent the value of actions regardless of the specific attributes that might contribute to value and typically do not represent isolated attributes.

For example, when choices are made via eye-movements (a saccade toward a selected alternative), the activity of saccade-selective neurons covaries with the value associated with the target. Such action values have been identified in numerous decision-related oculomotor structures including the lateral intra-parietal area (LIP) (Platt and Glimcher 1999, Sugrue et al. 2004).[32] The activity of LIP neurons correlates with the subjective value of potential saccades, whether this value is determined by sensory contingencies, reward magnitude and probability, delay discounting, foraging requirements, social information, or strategic valuation in a competitive game.[33] Thus, action-selective neurons — that typically project directly or indirectly to the circuits that implement a particular choice — encode the integrated subjective values of their associated actions. A number of recent fMRI studies, performed with human subjects implementing choices on a keyboard, also suggest that value signals from medial prefrontal regions are accumulated and compared during the choice process in dorso-lateral cortex and the intraparietal sulcus (Basten et al. 2010, Hare et al. 2011b, Domenech et al. 2017). Formally, this process can be modelled by appending a stochastic error term $\boldsymbol{\eta} = [\eta_1, \ldots, \eta_N] \in \mathbb{R}^N$ to valuations constructed in the first stage as in Equation (3). See Webb (2019) for more detail.

A.4. Summary

We are guided to the above formulation of a choice model by two key observations from the neurobiological literature. First, both human-imaging and electrophysiological evidence is consistent with binary choice decisions being implemented via a stochastic, dynamic, accumulation of value information in dorso-lateral and parietal cortex. Second, the electrophysiological evidence for divisive normalization in valuation tasks has been observed in the *same* brain regions, suggesting the divisive normalization computation is implemented prior to, or in conjunction with, this second-stage accumulation. Our aim is to model the transformation of valuations in this second stage. We therefore interpret $\mathbf{v}$ as a decision-maker's independent valuation of a consumer good, however constructed, and study the choice behaviour implied when these valuations are normalized in the implementation of a decision via $z(\mathbf{v})$ and the stochastic process captured by $\boldsymbol{\eta}$.

Again, we strongly suspect that the brain implements relative coding in earlier stages of the decision-making process — for instance in the construction of $\mathbf{v}$ from objective sensory attributes, perhaps in regions of orbito- and pre-frontal cortex. Electrophysiological evidence for adaptive coding in orbito-frontal regions can be found in the work of Padoa-Schioppa (2009). Chau et al. (2014) provide some initial fMRI evidence, though see Gluth et al. (2018). At the behavioural level, Landry and Webb (2019) and Noguchi

Figure A.4. (Color online) Conceptual Model of Two-Stage Decision Process in the Human Brain

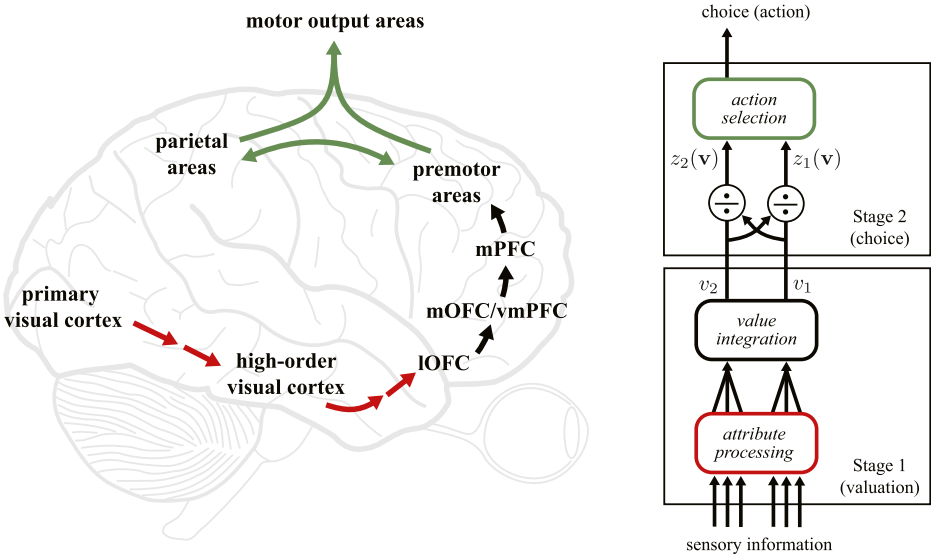

Notes. The colored arrows (left) reflect the temporal flow of information through these stages (right), rather than direct connectivity. Subcortical pathways are not depicted.

and Stewart (2018) provide reviews of the modelling literature in Economics and Psychology which implement relative coding at the level of attributes. The interaction of relative coding at multiple stages of the decision-making process, and how these representations interact to shape the form of context-dependent preferences, remains an exciting area for further research.

Appendix B. Closed-Form Results for Divisive Normalization

We now explore some formal properties of the Divisive Normalization model when the error density is given by the Gumbel distribution. The tractability of this distribution yields clear theoretical results for violations of regularity and membership in the class of set-dependent Luce models (Marley et al. 2008).

B.1. Divisive Normalization and Regularity

First, we find that Divisive Normalization will technically violate the regularity condition for some, but not all, values and parameterizations of the model. Our proof focuses on the Gumbel distribution because it has closed-form probabilities. We have not yet characterized the entire range of distributions and range of valuations for which regularity fails, but extensive simulation suggests it is small.

We begin with a definition of Random Utility. Let $P_{i,N}$ denote the probability that a subject chooses alternative i from a finite set N.

Definition B.1 (Random Utilities)**.** There exists a random vector $U = (U_1, \ldots, U_n)$, unique up to an increasing monotone transformation such that for any $i \in M \subseteq N$,

$$Pr\{U_i \geq U_j, \forall j \in M\} = P_{i,M}.$$

A necessary condition for a random utility representation states that the probability of choosing an alternative decreases as more alternatives are added to the choice set (Block and Marschak 1959), often referred to as a *regularity condition*.

Definition B.2 (Regularity)**.** If $L \subseteq M \subseteq N$,

$$P_{i,M} \leq P_{i,L}.$$

We now show that a model with normalization violates the regularity condition for some parameter values, therefore cannot be rationalized by a Random Utility model. We consider two choice sets of different sizes, the three alternative choice set {1,2,3}, with corresponding valuations $v_1 \geq v_2 \geq v_3 \geq 0$, and the two alternative subset {1,2}. Because we are assuming a Gumbel distribution, the choice probabilities of the normalized model are given by the closed-form equation,

$$P_{i,M} = \frac{e^{\omega \frac{v_i}{\sum_{n \in M} v_n}}}{\sum_{m \in M} e^{\omega \frac{v_m}{\sum_{n \in M} v_n}}}. \tag{B.1}$$

We will focus on the probability of choosing the second (ranked) alternative from the set. For our simple choice sets, these probabilities can be rewritten

$$P_{2,\{1,2,3\}} = \frac{1}{e^{\omega \frac{v_1 - v_2}{(v_1 + v_2 + v_3)}} + e^{\omega \frac{v_3 - v_2}{(v_1 + v_2 + v_3)}} + 1},$$

and

$$P_{2,\{1,2\}} = \frac{1}{e^{\omega \frac{v_1 - v_2}{(v_1 + v_2)}} + 1}.$$

We will show regularity is violated as the choice set is expanded from two to three alternatives.

Proposition B.1. There exists some $\bar{\omega} > \underline{\omega} \geq 0$ such that the choice probabilities:

1. Are regular for all $\omega > \bar{\omega}$ and therefore can be represented by Random Utilities.
2. Are not regular for all $\omega < \underline{\omega}$ and therefore cannot be represented by Random Utilities.

Proof. Part 1 requires that there is some $\bar{\omega} \geq 0$ such that $P_{2,\{1,2,3\}} < P_{2,\{1,2\}}$ if $\omega > \bar{\omega}$. Note that $P_{2,\{1,2,3\}} < P_{2,\{1,2\}}$ if and only if

$$e^{\frac{v_1-v_2}{\omega(v_1+v_2+v_3)}} + e^{\frac{v_3-v_2}{\omega(v_1+v_2+v_3)}} + 1 > e^{\frac{v_1-v_2}{\omega(v_1+v_2)}} + 1$$
$$e^{\frac{v_1-v_2}{\omega(v_1+v_2+v_3)} - \frac{v_1-v_2}{\omega(v_1+v_2)}} + e^{\frac{v_3-v_2}{\omega(v_1+v_2+v_3)} - \frac{v_1-v_2}{\omega(v_1+v_2)}} > 1$$
$$e^{-\frac{(v_1-v_2)v_3}{\omega(v_1+v_2)(v_1+v_2+v_3)}} + e^{-\frac{v_1^2+v_1v_2-2v_2v_3}{\omega(v_1+v_2)(v_1+v_2+v_3)}} > 1.$$

Because $v_1^2 + v_1v_2 - 2v_2v_3 > 2v_1v_3 - 2v_2v_3 > (v_1 - v_2)v_3 \geq 0$, the above expression is true if $e^{-\frac{v_1^2+v_1v_2-2v_2v_3}{\omega(v_1+v_2)(v_1+v_2+v_3)}} > \frac{1}{2}$, or equivalently,

$$\omega > \frac{1}{-\log\left(\frac{1}{2}\right)}\left(\frac{v_1^2 + v_1v_2 - 2v_2v_3}{(v_1+v_2)(v_1+v_2+v_3)}\right) > 0.$$

Part 2 requires that there is some $\bar{\omega} \geq 0$ such that $P_{2,\{1,2,3\}} < P_{2,\{1,2\}}$ if $\omega < \underline{\omega}$. Reversing the inequality (and argument) from above, $P_{2,\{1,2,3\}} < P_{2,\{1,2\}}$ if $e^{-\frac{(v_1-v_2)v_3}{\omega(v_1+v_2)(v_1+v_2+v_3)}} < \frac{1}{2}$, or equivalently,

$$\omega < \frac{1}{-\log\left(\frac{1}{2}\right)}\left(\frac{(v_1 - v_2)v_3}{(v_1+v_2)(v_1+v_2+v_3)}\right) > 0. \quad \square$$

Note that this result has an important qualification, namely regularity violations are only present for certain values of ω. This means that, for a subject with a given ω, there are only certain subsets of choice sets in which we should expect to see regularity violations. In particular, these violations will be more likely when v_3 and ω are both small.

B.2. Divisive Normalization and Set-Dependent Luce Models

Marley et al. (2008) introduced a class of *set-dependent Luce Models*, in which choice can be represented by a positive scale $b(i)$ and a positive scale $\phi(M)$ on choice sets $M \subseteq N$, where

$$P_{i,M} = \frac{b(i)^{\phi(M)}}{\sum_n b(n)^{\phi(M)}}.$$

In particular, such a representation holds if the choice probabilities satisfy two conditions. The first, originally described by Marley et al. (2008), requires that the choice ratios for any two alternatives vary over sets by a constant ratio.

Definition B.3. Set-Dependent Constant Ratio Rule

$$\frac{\log\frac{P_{i,L}}{P_{j,L}}}{\log\frac{P_{i,M}}{P_{j,M}}} = \frac{\log\frac{P_{k,L}}{P_{l,L}}}{\log\frac{P_{k,M}}{P_{l,M}}}, \tag{B.2}$$

for all $i, j, k, l \in L \cap M$ where $L \subseteq N$, and $M \subseteq N$.

The second necessary condition imposes monotonicity on the choice probabilities, as noted by Steverson et al. (2019):

Definition B.4. Ordering

$$P_{i,L} > P_{j,L} \text{ if and only if } P_{i,M} > P_{j,M}, \tag{B.3}$$

for all $i, j \in L \cap M$, where $L \subseteq N$, and $M \subseteq N$.

It is straightforward to show that a Divisive Normalization model (with Gumbel errors) satisfies both conditions. Working from Equation (B.1), Divisive Normalization maintains ordering in the choice probabilities because $P_{i,M} > P_{j,M}$ if and only if $v_i > v_j$ if and only if $P_{i,L} > P_{j,L}$. Moreover,

$$\log\frac{P_{i,L}}{P_{j,L}} = \frac{v_i - v_j}{\omega \sum_{n\in L} v_n}.$$

Therefore, Condition (B.2) reduces to $\frac{\omega \sum_{n\in M} v_n}{\omega \sum_{n\in L} v_n} = \frac{\omega \sum_{n\in M} v_n}{\omega \sum_{n\in L} v_n}$, thus is independent of the particular alternatives.

Appendix C. Within-Subject Estimation Results of Trinary Experiment

The normalization model can also be analyzed at the level of each subject to gauge heterogeneity in context-dependent choice behaviour. For example, when a subject faces a choice set in which the value of alternative 3 is large, we should expect to see a smaller ratio of alternative 1 chosen relative to alternative 2. A simple median split of the choice sets (per subject) confirms this intuition. The ratio $\frac{\hat{P}_1}{\hat{P}_2}$ is smaller for the upper median of b_3 for 34 of 40 subjects, with 13 of them significantly smaller at the 0.05 level.

Divisive Normalization also yields a prediction about *how much* context-dependent choice behaviour we should observe for a given range of choice sets. If v_1 and v_2 are far apart or if v_3 varies by a lot we should expect the choice effects of divisive normalization to be strong. In contrast, if v_1 and v_2 tend to be close together, or if v_3 does not vary by much, then we should expect them to be weak. Therefore, heterogeneity in the distribution of valuations that each subject placed on individual items can be used as an additional test of the model.

We assessed this prediction with two methods. Figure C.1 reports the maximum likelihood point estimates of the normalization model (7) for each subject. We report the estimate $\hat{\omega}$ multiplied by the average value of the choice set to give a sense of scale relative to $\hat{\sigma}$.[34] There is strong evidence for normalization in over half of the subject sample (21/40 subjects at the 0.10 level, 17/40 subjects at a 0.05 level). However, heterogeneity in the sample is clearly present in these subject-level point estimates, with the model assigning variance to either σ (red) or to the normalization term governed by ω (blue).

To assess this degree of heterogeneity, we conducted a hierarchical Bayesian analysis that assigns a probability to each subject belonging to one of two clusters. For each cluster $c \in 1, 2$, the normalization parameters (σ, ω, and β) are each drawn from a Gamma distribution with hyperparameters a_c and d_c (scale and shape, respectively).[35] The posterior density of the normalization parameters, for each subject, reflects the probability that the subject belongs to each of these clusters multiplied by the Gamma density for each cluster, thus how likely a given parameter value generated the data. Figure C.2 reports the posterior density for ω for each of the subjects. Out of the 40 subjects in the

Figure C.1. (Color online) Point Estimates, Logistic Analysis, and Range of Bids

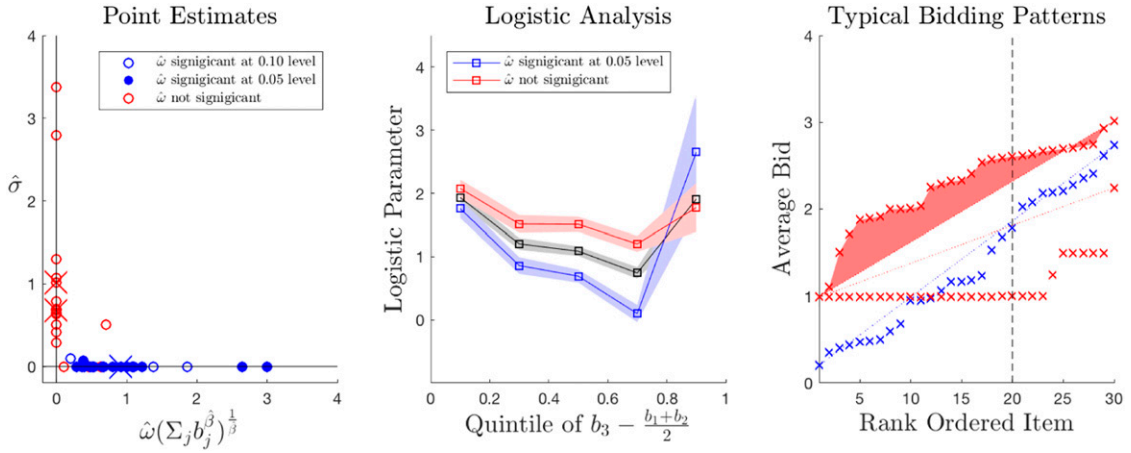

Notes. (Left) The point estimates of σ versus ω for each subject. (Middle) A logistic analysis reestimated for subsamples of subjects. The pooled analysis from Section 4.1.2 is reported in black. (Right) The range of bids for the set of items (shown for the three subjects denoted with an '×' in the left panel). The red polyhedron depicts the departure of the observed bids (for one subject) from a line between the minimum and maximum bid.

sample, we find that the posteriors place more weight on $\omega > 0.05$ then on $\omega < 0.05$ for 28 of the 40 subjects (in blue). Moreover, these are also the same subjects identified via the subject-specific point estimates (corr = 0.47, $p < 0.002$). Notably, the differences between the clusters arise primarily in the hyperparameter densities for ω, suggesting that the model is separating the clusters based on the degree of normalization evident in the choice probabilities (Figure C.3).

The implications of this heterogeneity in the choice probabilities can be visualized if we repeat the logistic analysis from Louie et al. (2013) on subsamples of subjects for which the point estimates $\hat{\omega}$ are significant or not (Figure C.1(b)). The subset of subjects that yield a significant $\hat{\omega}$ exhibit a strong contextual effect on the choice probabilities, in contrast to the remaining subjects in which the effect on choice probabilities is much weaker. Results are similar

Figure C.2. (Color online) Posterior Density of $\hat{\omega}$, for Each Subject, Estimated via a Hierarchical Bayesian Analysis

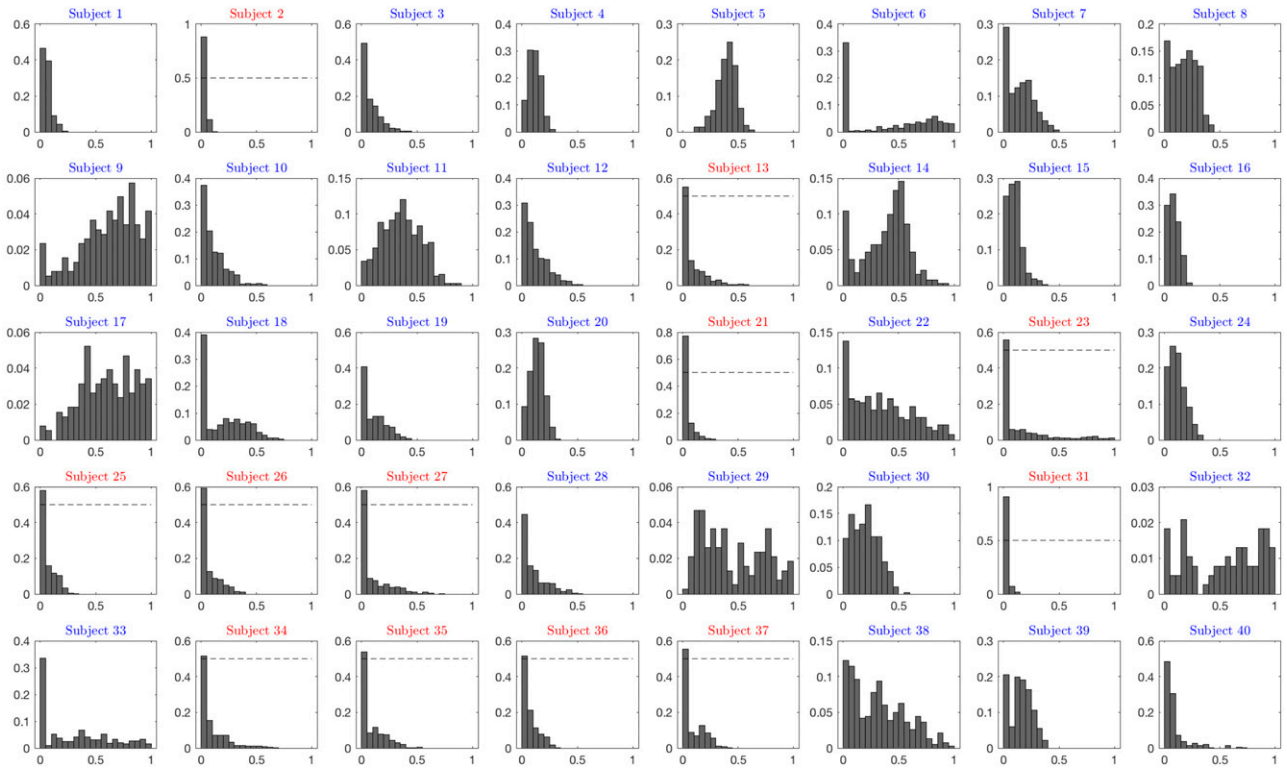

Note. The posteriors for subjects coded in blue place more density on $\hat{\omega} > 0.05$ and red place more density on $\hat{\omega} < 0.05$.

Figure C.3. (Color online) Posterior Densities of the Hyperparameters

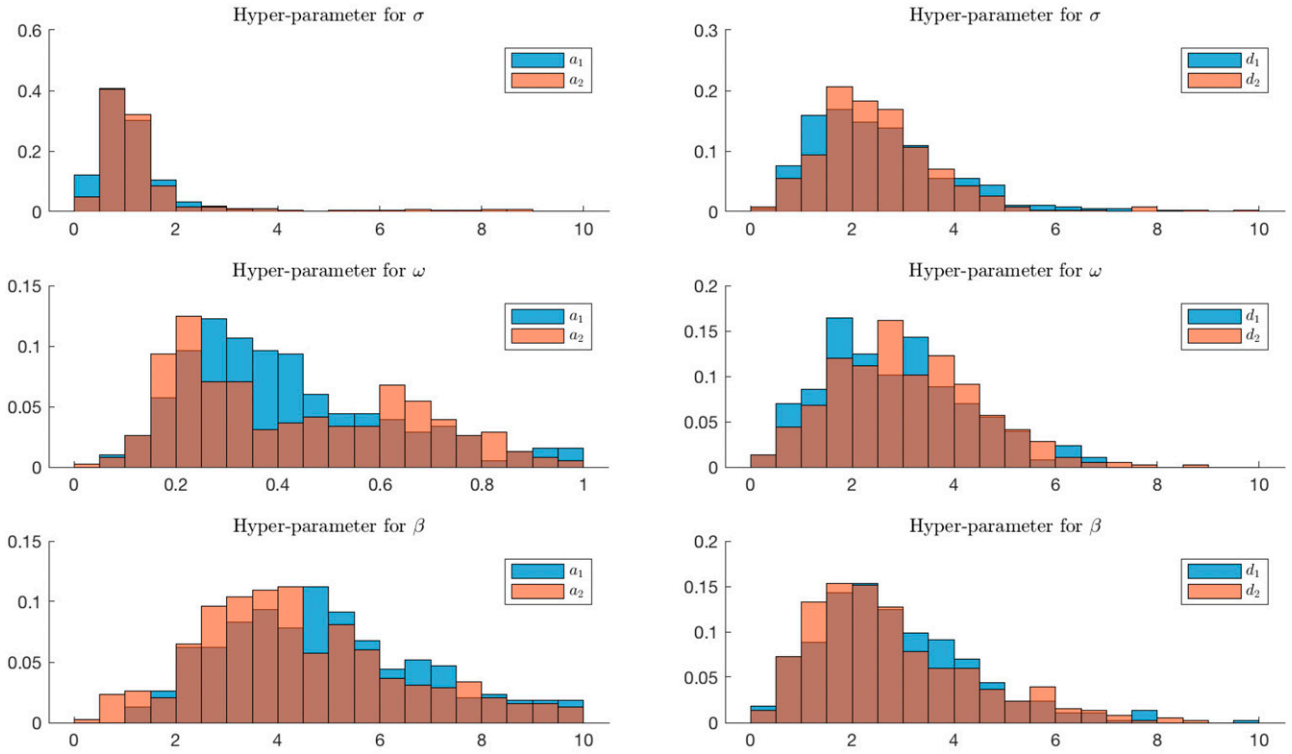

Notes. (Left) a_c scale, (right) d_c shape. From two clusters c for σ, ω, and β drawn from the distribution $\Gamma(a_c, d_c)$.

both if we split the sample at the 0.10 level and if we split it by the threshold on posterior densities identified by the hierarchical analysis in Figure C.2.

How might this heterogeneity in substitution patterns relate to the underlying bids? In Figure 18.C we highlight the ordered bids of three subjects, two of which with estimates of $\hat{\omega} \approx 0$ (in red). One of these subjects has a small range of bids for alternative 3 (b_3), and the other has a small range of bids for alternative 1 and 2 (b_1, b_2), relative to the subject with $\hat{\omega} > 0$ (in blue). Note that the bid spectrum of this latter subject has roughly equal range for both distractors and targets and therefore is roughly linear compared with the subjects with small $\hat{\omega}$.

To test this possible explanation for the heterogeneity we observe in our subject sample, we constructed a measurement of how much variation is present in valuations of the item set. For each item, we calculated the square of the difference between the rank-ordered valuations and a line that ranges from the minimum bid to the maximum bid. A subject for which the target and distractor set shared a similar range would exhibit a small measurement of variation and a large amount of normalization. A subject for which either the low-value items or high-value items yielded differing ranges of valuations would exhibit a large measurement and little normalization. We then averaged this metric over the two subsets of subjects defined by our regression results and found it was significantly larger ($p = 0.041$, two-sample t-test, two-tailed) for those subjects that did not exhibit normalization. This suggests that the small estimates of $\hat{\omega}$ we observed for some subjects resulted from a set of choice alternatives that were not conducive

Table D.1. Snack Food Items Presented to Subjects

Almond Joy candy bar
Cashews (whole salted)
Cheez-It baked snack crackers
Combos baked snacks
Cracker Jack (caramel popcorn)
Doritos tortilla chips (cool ranch)
Duke's beef jerky (teriyaki flavor)
Frito's corn chips
Goldfish baked snack crackers
Goobers chocolate coated peanuts
Haribo Gold-Bears gummi candy
Jelly Belly jelly beans
Jujyfruits candy
Kit Kat Extra Crispy candy bar
Lay's Barbecue potato chips
Milk Duds (chocolate and caramel)
M&M's chocolate candy
Oreo cookies
Planter's Peanut Bar candy bar
Pringles potato crisps
Raisinets chocolate raisins
Reese's Peanut Butter Cups
Ritter Sport chocolate bar
Ruffles potato chips
Smartfood popcorn (white cheddar)
Snickers candy bar
Sour Patch Kids candy
Swedish Fish candy
Toblerone chocolate bar
Twizzlers candy

Figure D.1. (Color online) Two Examples of Item Images Presented to the Subject During the Experiment

to generating choice set effects (for those subjects). Put another way, Divisive Normalization predicts that we should not expect to see choice set effects in those subjects.

Appendix D. Consumer Goods Used in Experiment

Appendix E: Relaxing the Semisaturation Parameter

Relaxing the assumption that $\sigma = 0$ reintroduces monotonicity into the transformed values (Figure E.1). For a given $\sigma > 0$, choice sets with lower total valuations are mapped to a line that intercepts lower than $1/\omega$.

$$\sum_i z_i = \sum_i \frac{v_i}{\sigma + \omega \sum_n v_n} = \frac{\sum_i v_i}{\sigma + \omega \sum_n v_n} < \frac{1}{\omega}. \qquad \text{(E.1)}$$

With a positive σ, the length of the vector $\mathbf{z}$ now depends monotonically on the length of the vector $\mathbf{v}$. This yields the prediction that choice errors are reduced for more valuable choice sets than for less valuable chose sets. However, choice errors increase relative to the case in which $\sigma = 0$; therefore, it seems that a neural system for decision-making

Figure E.2. Scaling Implemented by Normalization When $\sigma > 0$

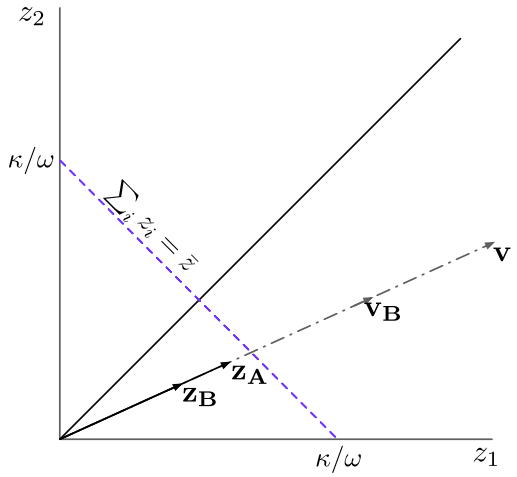

in *static choice environments* should have a σ near 0 (at least in the case of a constant variance for η). There is reason to believe this might not be the case in dynamic choice environments in which an average estimate of the choice set, or reference point, can prove useful for achieving optimal choice, suggesting that σ may, in fact, be a dynamic variable which varies with expectations.

Endnotes

[1] In a stochastic setting, Rieskamp et al. (2006) refer to Weak Stochastic Transitivity of choice probabilities as "perhaps the weakest bound on rationality." The model proposed here satisfies Weak Stochastic Transitivity.

[2] The recent literature on *rational inattention*, for example, examines how constraints on information processing (Shannon 1948) can explain observed departures from expected utility and the random utility model (Woodford 2012, Caplin and Dean 2015, Steiner and Stewart 2016, Khaw et al. 2017, Steverson et al. 2019, Frydman and Jin 2019).

[3] Using a metaphorical principal-agent environment to mimic evolutionary forces, they demonstrated that the optimal value function must be adaptive and depend on the distribution of alternatives in the choice set. In particular, maximum discriminability occurs where rewarding alternatives are most likely. Li et al. (2017) demonstrate this result numerically for a class of bounded functions. Robson and Whitehead (2019) describe the welfare implications of an adaptive utility. See also Alonso et al. (2014) for an argument for why an optimal allocation of neural resources might be bounded.

[4] This form of normalization has been previously studied in the sensory perception literature (Lyu and Simoncelli 2008, Lyu 2011, Sinz and Bethge 2013, Ballé et al. 2016a, Iyer and Burge 2018). Its role is to remove high-order correlations from natural stimuli (e.g., Ballé et al. 2016b). Typical implementations of normalization consider a range for β between 2 and 3 in sensory systems. See Appendix A.1 for more detail.

[5] The term "structural" is used in the econometrics literature to describe whether a model is imposed on the data for the purposes of estimating parameters that are believed to be invariant and informative, in contrast with a "reduced-form" analysis that places as few modelling assumptions on the data as possible (such as examining summary statistics). In cognitive psychology, it is much more common to build and estimate "process" models (what economists might call "structural" models).

[6] Building on prior work by Swait and Marley (2013) that relates Shannon entropy to a generalized Logit, Steverson et al. (2019) develop a normative foundation for Divisive Normalization by optimizing the tradeoff between the cost of errors and the cost of reducing stochasticity.

[7] Formally, we are assuming that a bid b_i is a strictly monotonic function of the underlying valuation v_i. Neural correlates of willingness-to-pay measures in prefrontal brain regions are described by Plassmann et al. (2007) and Chib et al. (2009).

[8] The fundamental feature of this, and a number of other models in the literature, is an aggregation and transformation of attribute information into a decision variable for each alternative (e.g., Trueblood et al. 2014, Tsetsos et al. 2010, Noguchi and Stewart 2018, Daviet 2018, Gluth et al. 2018). The simple model of value normalization presented here cannot mimic some features of these attribute-based models. For example, if $v_1 > v_2 > v_3$, then $z_1(\mathbf{v}) > z_2(\mathbf{v})$ for all values of v_3; therefore, the ordering of alternatives can never switch (we discuss violations of the Regularity axiom further in Appendix B). We believe a choice model with multiple stages of normalization is of great interest; see Zimmermann et al. (2018) for an initial example how multiple normalization stages might be related.

[9] The prevailing models of the comparison stage of the decision process (e.g., the *drift diffusion model*, Ratcliff 1978) have been shown to yield a stochastic additive formulation (Webb 2019). Moreover, this

process determines the density $f(\boldsymbol{\eta})$. For instance, it is broadly observed that as neural activity increases, the signal-to-noise ratio of decoded neural quantities also increases (e.g., McAdams and Maunsell 1999, Churchland et al. 2011). This is important because of a vast literature documenting that individual neural responses are approximately Poisson-like in their activity (Tolhurst et al. 1983). In terms of our model, this implies that the variance of $\boldsymbol{\eta}$ should not scale too strongly with $\mathbf{v}$, else choice might become *more* stochastic as valuations increase. Indeed, we will see that normalization can be interpreted as a specification of the variance of a choice model, thus imposes strong, testable, implications on choice data.

[10] Weber's law states that the change in a stimulus that will be *just noticeable* forms a constant ratio with the original stimulus. Consider Weber's original experiment. Each subject is given a 1 kg sack of sand, referred to as the reference stimulus, then given a second "test" sack and asked to choose which is heavier. As the weight of the test sack increases, the likelihood that subjects choose the test sack increases. Now the experiment is repeated with a 10 kg reference sack. Weber found that the range of weights over which subjects make an error increases in proportion to the weight of the reference sack.

[11] Our focus on choice errors follows the economic literature that has previously used errors as a metric of optimality (Robson 2001a, Rayo and Becker 2007, Robson and Samuelson 2010). Whereas we do not argue explicitly in terms of the evolutionary criteria of "expected loss," which incorporates the magnitude of a choice error (Netzer 2009), in the appendix we show that the general divisive normalization computation does allow a degree of monotonicity in the transformation of subjective values, such that "more valuable" choice sets (in the sense that $\alpha\mathbf{v}$ is more valuable than $\mathbf{v}$ if $\alpha > 1$) will lead to fewer errors than less valuable choice sets. Of course, a full normative treatment of the neural decision-making problem would require a complete accounting of the costs of decision-related errors to the chooser and the metabolic costs of relaxing the constraints we identify — on an evolutionary timescale.

[12] Other examples of models that use local range normalization include Wilcox (2011).

[13] A restricted form of normalization model rectifies the unboundedness problem by setting $\min[\mathbf{v}] = 0$ (e.g., González-Vallejo 2002). This model also provides a link between range normalization and divisive normalization. To see how, recall that as $\beta \to \infty$, the β-norm converges to a maximization. Therefore, $z_i(\mathbf{v}) \propto \frac{v_i}{(\sum_n v_n^\beta)^{\frac{1}{\beta}}} \to \frac{v_i}{\max[\mathbf{v}]}$. The divisive normalization computation therefore simplifies to this restricted form when β is large.

[14] Briefly, to realize a bid trial, subjects drew a chip from a bag containing chips numbered from \$0–\$4 in \$0.10 increments; the drawn number determined the price p of the item in that trial and was compared with the bid b. If $b \geq p$, the subject received the item for the price p; if $b < p$, the subject paid nothing and did not receive the item. Thus, it is generally considered incentive-compatible for a subject to report their maximal willingness to pay because they cannot influence the price. Subjects were carefully informed of this property of the BDM auction in the initial instructions and practiced it before the actual experiment. At the conclusion of the experiment, a single trial from the session (bid or choice) was randomly selected for realization and the subject received their choice on that trial. In addition, each subject received a \$40 show-up fee.

[15] The weak relationship between b_2 and $\hat{P}_2$ is a property of the experimental design. Since $b_2 < b_1$ by definition, b_1 tends to be larger as b_2 increases, limiting any increase in the observed frequency of choosing the second alternative, $\hat{P}_2$.

[16] This result is robust to the two outlier subjects with small average $\tilde{b}_3$.

[17] The multivariate normal distribution is parameterized with the constant variance term σ and the Cholesky factorization of the covariance matrix, differenced with respect to the first alternative, $\begin{pmatrix} 1 & 0 \\ l_{2,1} & l_{2,2} \end{pmatrix}$.

[18] Each specification is estimated via Maximum Likelihood with bound constraints to ensure that the parameters σ, ω, and β were nonnegative.

[19] To test the importance of the normal density assumption, we also examined a Divisive Normalization model ($\omega \geq 0$) in which $f()$ is the Gumbel density (not reported in Table 1). We find that $\hat{\omega}$ is significantly different from zero with a log-likelihood of −7999.58. However, it is the worst performing normalization specification, likely because of the fact that it cannot capture the shape of the $\frac{p_1}{p_2}$ ratio (Figure 5).

[20] The LR statistic is calculated from the simple normalization model (with $\beta = 1$). In the specification with an unrestricted covariance matrix we cannot reject the hypothesis that $\beta = 1$ ($p = 0.09$, LR Test).

[21] Formally, there is a ridge in the log-likelihood function for values of β larger than ~ 10, which makes the point estimate of a large β imprecise. Some intuition can be found in Figure 3. As β varies, there is little change in the geometric shape implied by normalization (e.g., a normalization boundary just inside the square would imply only a small change in z_1 and z_2). This implies only a small change in the resulting choice probabilities as the estimator varies β. To calculate the standard errors of $\hat{\omega}$ and $\hat{\sigma}$ in this specification, we hold $\hat{\beta}$ fixed at the reported estimate, which yields a likelihood ratio statistic $\chi^2(LR, 1) = 0.05$. All reported hypothesis tests on normalization parameters are based on a likelihood ratio (LR) test statistic, not the reported standard errors.

[22] In Appendix C we also consider a hierarchical model where each parameter is drawn from a distribution belonging to one of two clusters of subjects.

[23] The increase in the predicted probability of choosing alternative 3 arises from the construction of our choice set. Alternatives 3–12 were randomly sampled from a set of 10 items, which means that smaller choice sets were more likely to have a larger disparity between alternative 3 and the remaining alternatives.

[24] As noted earlier, interpreting the results from the Probit estimation may be problematic because its estimation is inconsistent in the presence of Divisive Normalization.

[25] There is a large literature in neuroscience and psychology that examines the prevalence of errors as a function of the time spent on a decision, known as the *speed/accuracy trade-off* (for a review, see Bogacz et al. 2010). This literature finds that one can improve accuracy with longer decision times but that this increase in accuracy is bounded. The fact that increasing the time devoted to a decision cannot overcome this resource limitation problem reflects a temporal constraint that has been both widely observed and biologically explained, though is not the subject of this article.

[26] We should note that the normalization model describes a computational algorithm rather than a specific biophysical implementation. Researchers have identified a number of potential neural mechanisms for implementing normalization and it is likely that the normalization computation is mediated by different processes in different species and systems. Moreover, because evolution selects on the fitness of the output of a particular neural system, the parametrization of the normalization equation will depend on the role of the particular system and statistical features of its input. The widespread occurrence and varying implementations indicate that it is the normalization computation rather than the specific mechanism and/or parameterization, which is critical to efficient neural systems.

[27] In particular, frontal brain regions receive prominent projections from the amygdala and posterior granular orbital insula (Porrino et al. 1981, Carmichael and Price 1996), brain regions involved in processing reward information and olfactory, gustatory, and visceral sensory information, respectively. Frontal brain regions also send projections to the ventral striatum, one of the core brain regions identified in functional neuroimaging studies as representing the subjective valuation of choice alternatives (Bartra et al. 2013).

[28] This evidence extends beyond human fMRI to direct observation of neural activity via electrophysiological recording. Neurons in the monkey orbitofrontal cortex represent the economic value of options at the time of decision-making (Padoa-Schioppa and Assad 2006, Padoa-Schioppa and Conen 2017)

[29] In addition, lesion studies in both monkeys (Rudebeck et al. 2017, Izquierdo 2004) and humans (Noonan et al. 2017, Camille et al. 2011) demonstrate that frontal brain regions are necessary for value-guided choice behaviour.

[30] In primate experiments, neural activity in orbito-frontal cortex also correlate with value and choice information. This has led to the hypothesis that decisions can also occur in an action-independent framework, with choices made between options independent of the particular motor action used to implement choice (Padoa-Schioppa 2011, Cai and Padoa-Schioppa 2014), or perhaps in conjunction with action-selective regions (Cisek 2012, Padoa-Schioppa and Conen 2017). Our model of value normalization is consistent with either interpretation; it simply requires a hypothesis about the brain region in which the normalization computation is operating. The same model would describe goods-based choice as long as the neurons that actually implement a selection process receive normalized inputs. The critical hypothesis is that normalization takes place over options regardless of whether the values are coded in an action-dependent or -independent framework.

[31] In particular, decision-related activity has been identified in high-level sensory association areas in parietal cortex, premotor cortical brain regions, and subcortical structures such as the striatum and superior colliculus.

[32] Similar results have been observed in the frontal eye fields (Ding and Hikosaka 2006), the superior colliculus (Ikeda and Hikosaka 2003), and the caudate nucleus in the striatum (Samejima 2005)

[33] Shadlen and Newsome (2001), Roitman and Shadlen (2002), Louie and Glimcher (2010), Platt and Glimcher (1999), Dorris and Glimcher (2004), Klein et al. (2008), and Sugrue et al. (2004)

[34] The statistical significance of the estimate $\hat{\omega}$ is calculated via a likelihood ratio test from the restricted model with $\omega = 0$.

[35] We conducted analyses with both a uniform prior and a prior that places substantial density on $\omega = 0$. Results were similar in both cases, suggesting that the prior has limited effect on the results (we report results for the "uninformative" prior). The uninformative prior has the benefit of allowing the posterior to be interpreted as the likelihood, thus providing a conceptual link to frequentist analysis.

References

Alonso R, Brocas I, Carrillo JD (2014) Resource allocation in the brain. *Rev. Econom. Stud.* 81(2):501–534.

Ballé J, Laparra V, Simoncelli EP (2016a) Density modeling of images using a generalized normalization transformation. Preprint, submitted February 29, https://arxiv.org/abs/1511.06281.

Ballé J, Laparra V, Simoncelli EP (2016b) End-to-end optimized image compression. Preprint, submitted November 5, https://arxiv.org/abs/1611.01704.

Barlow HB (1961) Possible principles underlying the transformation of sensory messages.Rosenblith WA, ed., Sensory Communication (MIT Press, Cambridge, MA).

Bartra O, McGuire JT, Kable JW (2013) The valuation system: A coordinate-based meta-analysis of BOLD fMRI experiments examining neural correlates of subjective value. *Neuroimage* 76:412–427.

Basso MA, Wurtz RH (1997) Modulation of neuronal activity by target uncertainty. *Nature* 389(6646):66–69.

Basten U, Biele G, Heekeren HR, Fiebach CJ (2010) How the brain integrates costs and benefits during decision making. *Proc. Natl. Acad. Sci. USA* 107(50):21767–21772.

Becker GM, DeGroot MH, Marschak J (1964) Measuring utility by a single-response sequential method. *Behav. Sci.* 9(3):226–232.

Bernheim BD (2009) On the potential of neuroeconomics: A critical (but hopeful) appraisal. *Amer. Econom. J. Microeconom.* 1(2):1–41.

Bhatia S, Stewart N (2018) Naturalistic multiattribute choice. *Cognition* 179:71–88.

Bhui R, Gershman S (2018) Decision by sampling implements efficient coding of psychoeconomic functions. *Psych. Rev.* 125(6): 985–1001.

Block HD, Marschak J (1959) Random orderings and stochastic theories of responses. Discussion Paper 66, Cowles Foundation for Research in Economics, Yale University, New Haven, CT.

Bogacz R, Wagenmakers EJ, Forstmann BU, Nieuwenhuis S (2010) The neural basis of the speed-accuracy tradeoff. *Trends Neurosci.* 33(1):10–16.

Bushong B, Schwartzstein J, Rabin M (2019) A model of relative thinking. Working paper, Michigan State University, East Lansing, MI.

Cai X, Padoa-Schioppa C (2014) Contributions of orbitofrontal and lateral prefrontal cortices to economic choice and the good-to-action transformation. *Neuron* 81(5):1140–1151.

Camara E, Rodriguez-Fornells A, Ye Z, Münte TF (2009) Reward networks in the brain as captured by connectivity measures. *Front. Neurosci.* 3(3):350–362.

Camille N, Griffiths CA, Vo K, Fellows LK, Kable JW (2011) Ventromedial frontal lobe damage disrupts value maximization in humans. *J. Neurosci.* 31(20):7527–7532.

Caplin A, Dean M (2015) Revealed preference, rational inattention, and costly information acquisition. *Amer. Econom. Rev.* 105(7): 2183–2203.

Carandini M, Heeger DJ (2012) Normalization as a canonical neural computation. *Nat. Rev. Neurosci.* 13(1):51–62.

Carandini M, Heeger DJ, Movshon JA (1997) Linearity and Normalization in Simple Cells of the Macaque Primary Visual Cortex. *J. Neurosci.* 17(21):8621–8644.

Carmichael ST, Price JL (1996) Connectional networks within the orbital and medial prefrontal cortex of macaque monkeys. *J. Comp. Neurol.* 371(2):179–207.

Chau BKH, Kolling N, Hunt LT, Walton ME, Rushworth MFS (2014) A neural mechanism underlying failure of optimal choice with multiple alternatives. *Nat. Neurosci.* 17(3):463–470.

Chib VS, Rangel A, Shimojo S, O'Doherty JP (2009) Evidence for a common representation of decision values for dissimilar goods in human ventromedial prefrontal cortex. *J. Neurosci.* 29(39): 12315–12320.

Churchland AK, Kiani R, Chaudhuri R, Wang XJ, Pouget A, Shadlen MN (2011) Variance as a signature of neural computations during decision making. *Neuron* 69(4):818–831.

Cisek P (2012) Making decisions through a distributed consensus. *Curr. Opin. Neurobiol.* 22(6):927–936.

Cisek P, Kalaska JF (2010) Neural mechanisms for interacting with a world full of action choices. *Annu. Rev. Neurosci.* 33(1):269–298.

Clithero JA, Rangel A (2013) Informatic parcellation of the network involved in the computation of subjective value. *Soc. Cogn. Affect. Neurosci.* 9(9):1–14.

Daviet R (2018) Methods for statistical analysis and prediction of discrete choices. PhD thesis, University of Toronto, Toronto, Ontario, Canada.

Debreu G (1960) Individual choice behavior: A theoretical analysis by R. Duncan Luce. *Amer. Econom. Rev.* 50(1):186–188.

Ding L, Hikosaka O (2006) Comparison of reward modulation in the frontal eye field and caudate of the macaque. *J. Neurosci.* 26(25): 6695–6703.

Domenech P, Redouté J, Koechlin E, Dreher JC (2017) The neuro-computational architecture of value-based selection in the human brain. *Cerebral Cortex* 28(2):1–17.

Dorris MC, Glimcher PW (2004) Activity in posterior parietal cortex is correlated with the relative subjective desirability of action. *Neuron* 44(2):365–378.

Fehr E, Rangel A (2011) Neuroeconomic foundations of economic choice—Recent advances. *J. Econom. Perspect.* 25(4):3–30.

FitzGerald THB, Seymour B, Dolan RJ (2009) The role of human orbitofrontal cortex in value comparison for incommensurable objects. *J. Neurosci.* 29(26):8388–8395.

Frydman C, Jin LJ (2019) Efficient coding and risky choice. Working paper, University of Southern California, Los Angeles.

Ganguli D, Simoncelli EP (2014) Efficient sensory encoding and Bayesian inference with heterogeneous neural populations. *Neural Comput.* 26(10):2103–2134.

Glimcher PW (2003) The neurobiology of visual-saccadic decision making. *Ann. Rev. Neurosci.* 26(1):133–179.

Glimcher PW (2005) Indeterminacy in brain and behavior. *Annu. Rev. Psych.* 56(1):25–56.

Glimcher PW (2011) *Foundations of Neuroeconomic Analysis* (Oxford University Press, Oxford, England).

Gluth S, Spektor MS, Rieskamp J (2018) Value-based attentional capture affects multi-alternative decision making. *eLife* 7(e39659).

Gold JI, Shadlen MN (2007) The neural basis of decision making. *Ann. Rev. Neurosci.* 30:535–574.

González-Vallejo C (2002) Making trade-offs: A probabilistic and context-sensitive Model of Choice Behavior. *Psych. Rev.* 109(1): 137–155.

Greene WH (2003) *Econometric Analysis*, 5th ed. (Prentice Hall, Upper Saddle River, NJ).

Hare TA, Malmaud J, Rangel A (2011a) Focusing attention on the health aspects of foods changes value signals in vmPFC and improves dietary choice. *J. Neurosci.* 31(30):11077–11087.

Hare TA, Schultz W, Camerer CF, O'Doherty JP, Rangel A (2011b) Transformation of stimulus value signals into motor commands during simple choice. *Proc. Natl. Acad. Sci. USA* 108(44):18120–18125.

Hartline HK, Ratliff F (1957) Inhibitory interaction of receptor units in the eye of Limulus. *J. General Physiol.* 40(3):357–376.

Hawkins GE, Forstmann BU, Wagenmakers EJ, Ratcliff R, Brown SD (2015) Revisiting the evidence for collapsing boundaries and urgency signals in perceptual decision-making. *J. Neurosci.* 35(6): 2476–2484.

Heeger DJ (1992) Normalization of cell responses in cat striate cortex. *Visual Neurosci.* 9(2):181–197.

Holper L, Van Brussel LD, Schmidt L, Schulthess S, Burke CJ, Louie K, Seifritz E, Tobler PN (2017) Adaptive value normalization in the prefrontal cortex is reduced by memory load. *eNeuro* 4(2):1–20.

Hubel DH, Wiesel TN (1968) Receptive fields and functional architecture of monkey striate cortex. *J. Physiol.* 195:215–243.

Huber J, Payne JW, Puto C (1982) Adding asymmetrically dominated alternatives: Violations of regularity and the similarity hypothesis. *J. Consum. Res.* 9(1):90–98.

Hunt LT, Hayden BY (2017) A distributed, hierarchical and recurrent framework for reward-based choice. *Nat. Rev. Neurosci.* 18(3): 172–182.

Ikeda T, Hikosaka O (2003) Reward-dependent gain and bias of visual responses in primate superior colliculus. *Neuron* 39(4): 693–700.

Iyer A, Burge J (2018) Model neuron response statistics to natural images. *bioRxiv* 7(2):387183.

Izquierdo A (2004) Bilateral orbital prefrontal cortex lesions in rhesus monkeys disrupt choices guided by both reward value and reward contingency. *J. Neurosci.* 24(34):7540–7548.

Kahneman D, Tversky A (1979) Prospect theory: An analysis of decision under risk. *Econometrica* 47(2):263–292.

Kennerley SW, Wallis JD (2009) Evaluating choices by single neurons in the frontal lobe: outcome value encoded across multiple decision variables. *Eur. J. Neurosci.* 29(10):2061–2073.

Khaw MW, Li Z, Woodford M (2017) Risk aversion as a perceptual bias. NBER Working Paper No. 23294, National Bureau of Economic Research, Cambridge, MA.

Klein JT, Deaner RO, Platt ML (2008) Neural correlates of social target value in macaque parietal cortex. *Current Biol.* 18(6):419–424.

Klein TA, Ullsperger M, Jocham G (2017) Learning relative values in the striatum induces violations of normative decision making. *Nat. Comm.* 8:16033.

Koszegi B, Rabin M (2006) A model of reference-dependent preferences. *Quart. J. Econom.* 121(4):1133–1165.

Krajbich I, Armel C, Rangel A (2010) Visual fixations and the computation and comparison of value in simple choice. *Nat. Neurosci.* 13(10):1292–1298.

Landry P, Webb R (2020) Pairwise normalization: A neuroeconomic theory of multi-attribute choice. Working paper, University of Toronto, Toronto, Ontario, Canada.

Levy D, Glimcher PW (2011) Comparing apples and oranges: Using reward-specific and reward-general subjective value representation in the brain. *J. Neurosci.* 31(41):14693–14707.

Levy DJ, Glimcher PW (2012) The root of all value: A neural common currency for choice. *Current Opinions Neurobiol.* 22(6): 1027–1038.

Li V, Castañón SH, Solomon JA, Vandormael H, Summerfield C (2017) Robust averaging protects decisions from noise in neural computations. *PLOS Comput. Biol.* 13(8):e1005723.

Lichtenstein S, Slovic P (2006) *The Construction of Preference* (Cambridge University Press, New York).

Lin A, Adolphs R, Rangel A (2012) Social and monetary reward learning engage overlapping neural substrates. *Soc. Cognitive Affective Neurosci.* 7(3):274–281.

LoFaro T, Louie K, Webb R, Glimcher PW (2014) The temporal dynamics of cortical normalization models of decision-making. *Lett. Biomath.* 1(2):209–220.

Louie K, Glimcher PW (2010) Separating value from choice: Delay discounting activity in the lateral intraparietal area. *J. Neurosci.* 30(16):5498–5507.

Louie K, Glimcher PW, Webb R (2015) Adaptive neural coding: From biological to behavioral decision-making. *Current Opinions Behav. Sci.* 5:91–99.

Louie K, Grattan LE, Glimcher PW (2011) Reward value-based gain control: Divisive normalization in parietal cortex. *J. Neurosci.* 31(29):10627–10639.

Louie K, Khaw MW, Glimcher PW (2013) Normalization is a general neural mechanism for context-dependent decision making. *Proc. Natl. Acad. Sci. USA* 110(15):6139–6144.

Louie K, LoFaro T, Webb R, Glimcher PW (2014) Dynamic divisive normalization predicts time-varying value coding in decision-related circuits. *J. Neurosci.* 34(48):16046–16057.

Louviere J, Street D, Carson R, Ainslie A, DeShazo JR, Cameron T, Hensher D, Kohn R, Marley AAJ (2002) Dissecting the random component of utility. *Marketing Lett.* 13(3):177–193.

Luce RD (1959) *Individual Choice Behaviour* (John Wiley, Hoboken, NJ).

Lyu S (2011) Dependency reduction with divisive normalization: Justification and effectiveness. *Neural Comput.* 23(11):2942–2973.

Lyu S, Simoncelli EP (2008) Nonlinear image representation using divisive normalization. *Conf. Computer Vision Pattern Recognition 2008* (Institute of Electrical and Electronics Engineers, Washington, DC), 1–8.

Machens CK, Gollisch T, Kolesnikova O, Herz A (2005) Testing the efficiency of sensory coding with optimal stimulus ensembles. *Neuron* 47:447–456.

Mainen ZF, Sejnowski TJ (1995) Reliability of spike timing in neocortical neurons. *Science* 268(5216):1503–1506.

Marley AAJ, Flynn TN, Louviere JJ (2008) Probabilistic models of set-dependent and attribute-level best–worst choice. *J. Math. Psych.* 52(5):281–296.

McAdams CJ, Maunsell JHR (1999) Effects of attention on orientation-tuning functions of single neurons in macaque cortical area V4. *J. Neurosci.* 19(1):431–441.

McFadden DL (2001) Economic choices. *Amer. Econom. Rev.* 91(3): 351–378.

McNamee D, Rangel A, O'Doherty JP (2013) Category-dependent and category-independent goal-value codes in human ventromedial prefrontal cortex. *Nat. Neurosci.* 16(4):479–485.

Moisa M, Polania R, Grueschow M, Lee YJ, Nagy Z, Ruff C (2018) A causal account of the brain network mechanisms underlying value-based choices. Annual Meeting, Society for Neuroeconomics, British Colombia, Canada.

Netzer N (2009) Evolution of time preferences and attitudes toward risk. *Amer. Econom. Rev.* 99(3):937–955.

Noguchi T, Stewart N (2018) Multialternative decision by sampling: A model of decision making constrained by process data. *Psych. Rev.* 125(4):512–544.

Noonan MP, Chau B, Rushworth MF, Fellows LK (2017) Contrasting effects of medial and lateral orbitofrontal cortex lesions on credit assignment and decision making in humans. *J. Neurosci.* 37(29): 7023–7035.

Ongür D, Price JL (2000) The organization of networks within the orbital and medial prefrontal cortex of rats, monkeys and humans. *Cerebral Cortex* 10(3):206–219.

Padoa-Schioppa C (2009) Range-adapting representation of economic value in the orbitofrontal cortex. *J. Neurosci.* 29(44): 14004–14014.

Padoa-Schioppa C (2011) Neurobiology of economic choice: A good-based model. *Annu. Rev. Neurosci.* 34(1):333–359.

Padoa-Schioppa C, Assad JA (2006) Neurons in the orbitofrontal cortex encode economic value. *Nature* 441(7090):223–226.

Padoa-Schioppa C, Conen KE (2017) Orbitofrontal cortex: A neural circuit for economic decisions. *Neuron* 96(4):736–754.

Pastor-Bernier A, Cisek P (2011) Neural correlates of biased competition in premotor cortex. *J. Neurosci.* 31(19):7083–7088.

Plassmann H, O'Doherty JP, Rangel A (2007) Orbitofrontal cortex encodes willingness to pay in everyday economic transactions. *J. Neurosci.* 27(37):9984–9988.

Platt ML, Glimcher PW (1999) Neural correlates of decision variables in parietal cortex. *Nature* 400:233–238.

Platt ML, Plassmann H (2013) *Muiltistage Valuation Signals and Common Neural Currencies. Neuroeconomics* (Academic Press, San Diego, CA).

Polania R, Moisa M, Opitz A, Grueschow M, Ruff CC (2015) The precision of value-based choices depends causally on fronto-parietal phase coupling. *Nat. Comm.* 6(1):8090.

Polania R, Woodford M, Ruff CC (2019) Efficient coding of subjective value. *Nat. Neurosci.* 22(1):134–142.

Porrino LJ, Crane AM, Rakic PSG (1981) Direct and indirect pathways from the amygdala to the frontal lobe in rhesus monkeys. *J. Comp. Neurol.* 198(1):121–136.

Qamar AT, Cotton RJ, George RG, Beck JM, Prezhdo E, Laudano A, Tolias AS, Ma WJ (2013) Trial-to-trial, uncertainty-based adjustment of decision boundaries in visual categorization. *Proc. Natl. Acad. Sci. USA*. 110(50):20332–20337.

Rangel A, Clithero JA (2012) Value normalization in decision making: Theory and evidence. *Curr. Opin. Neurobiol.* 22(6):970–981.

Ratcliff R (1978) A theory of memory retrieval. *Psych. Rev.* 85(2): 59–108.

Rayo L, Becker GS (2007) Evolutionary efficiency and happiness. *J. Political Econom.* 115(2):302–337.

Rich EL, Wallis JD (2016) Decoding subjective decisions from orbitofrontal cortex. *Nat. Neurosci.* 19(7):973–980.

Rieskamp J, Busemeyer JR, Mellers B (2006) Extending the bounds of rationality: Evidence and theories of preferential choice. *J. Econom. Literature* 44(3):631–661.

Robson AJ (2001a) The biological basis of economic behavior. *J. Econom. Literature* 39(1):11–33.

Robson AJ (2001b) Why would nature give individuals utility functions? *J. Political Econom.* 109(4):900–914.

Robson AJ, Samuelson L (2010) The evolutionary foundations of preferences. Benhabib J, Bisin A, Jackson M, eds. *Handbook of Social Economics* (North Holland, London), 221–310.

Robson AJ, Whitehead L (2019) Adaptive cardinal utility. Working paper, Simon Fraser University, Vancouver, British Columbia, Canada.

Roitman J, Shadlen MN (2002) Response of neurons in the lateral intraparietal area during a combined visual discrimination reaction time task. *J. Neurosci.* 22(21):9475–9489.

Rorie AE, Gao J, McClelland JL, Newsome WT (2010) Integration of sensory and reward information during perceptual decision-making in lateral intraparietal cortex (LIP) of the macaque monkey. *PLoS One* 5(2):e9308.

Rudebeck PH, Saunders RC, Lundgren DA, Murray EA (2017) Specialized representations of value in the orbital and ventrolateral prefrontal cortex: Desirability vs. availability of outcomes. *Neuron* 95:1208–1220.

Rust NC, Mante V, Simoncelli EP, Movshon JA (2006) How MT cells analyze the motion of visual patterns. *Nat. Neurosci.* 9(11): 1421–1431.

Salisbury LC, Feinberg F (2010) Alleviating the constant stochastic variance assumption in decision research: Theory, measurement, and experimental test. *Marketing Sci.* 29(1):1–17.

Samejima K (2005) Representation of action-specific reward values in the striatum. *Science* 310(25):1337–1340.

Schwartz O, Simoncelli EP (2001) Natural signal statistics and sensory gain control. *Nat. Neurosci.* 4(8):819–825.

Seymour B, McClure SM (2008) Anchors, scales and the relative coding of value in the brain. *Curr. Opin. Neurobiol.* 18(2):173–178.

Shadlen MN, Kiani R (2013) Decision making as a window on cognition. *Neuron* 80(3):791–806.

Shadlen MN, Newsome WT (1998) The variable discharge of cortical neurons: implications for connectivity, computation, and information coding. *J. Neurosci.* 18(10):3870–3896.

Shadlen MN, Newsome WT (2001) Neural basis of a perceptual decision in the parietal cortex (area LIP) of the rhesus monkey. *J. Neurophysiol.* 86(4):1916–1936.

Shadlen MN, Shohamy D (2016) Decision making and sequential sampling from memory. *Neuron* 90:927.

Shannon CE (1948) A mathematical theory of communication. *Bell Systems Tech. J.* 27(3):379–423.

Simon HA (1979) Rational decision making in business organizations. *Amer. Econom. Rev.* 69(4):493–513.

Simonson I (1989) Choice based on reasons: The case of attraction and compromise effects. *J. Consumer Res.* 16(2):158–174.

Sinz F, Bethge M (2013) Temporal adaptation enhances efficient contrast gain control on natural images. *PLOS Comput. Biol.* 9(1): e1002889.

Slovic P, Lichtenstein S (1983) Preference reversals: A broader perspective. *Amer. Econom. Rev.* 73(4):596–605.

Smith A, Bernheim BD, Camerer CF, Rangel A (2014) Neural activity reveals preferences without choices. *Amer. Econom. J. Microeconom.* 6(2):1–36.

Soltani A, De Martino B, Camerer CF (2012) A range-normalization model of context-dependent choice: A new model and evidence. *PLOS Comput. Biol.* 8(7):e1002607.

Steiner J, Stewart C (2016) Perceiving prospects properly. *Amer. Econom. Rev.* 106(7):1601–1631.

Stevens CF (2003) Neurotransmitter release at central synapses. *Neuron* 40(2):381–388.

Stevens SS (1961) To honor Fechner and repeal his law: A power function, not a log function, describes the operating characteristic of a sensory system. *Science* 133(3446):80–86.

Steverson K, Brandenburger A, Glimcher P (2019) Choice-theoretic foundations of the divisive normalization model. *J. Econom. Behav. Organ.* 164:148–165.

Sugrue LP, Corrado GS, Newsome WT (2004) Matching behavior and the representation of value in the parietal cortex. *Science* 304(5678):1782–1787.

Summerfield C, Tsetsos K (2012) Building bridges between perceptual and economic decision-making: Neural and computational mechanisms. *Frontiers Neurosci.* 6:70.

Suzuki S, Cross L, O'Doherty JP (2017) Elucidating the underlying components of food valuation in the human orbitofrontal cortex. *Nat. Neurosci.* 20(12):1780–1786.

Swait J, Marley AAJ (2013) Probabilistic choice (models) as a result of balancing multiple goals. *J. Math. Psych.* 57(1–2):1–14.

Tolhurst DJ, Movshon JA, Dean AF (1983) The statistical reliability of signals in single neurons in cat and monkey visual cortex. *Vision Res.* 23(8):775–785.

Train KE (2009) *Discrete Choice Methods with Simulation*, 2nd ed. (Cambridge University Press, New York).

Tremblay L, Schultz W (1999) Relative reward preference in primate orbitofrontal cortex. *Nature* 398(6729):704–708.

Trueblood JS, Brown SD, Heathcote A (2014) The multiattribute linear ballistic accumulator model of context effects in multialternative choice. *Psych. Rev.* 121(2):179–205.

Tsetsos K, Usher M, Chater N (2010) Preference reversal in multiattribute choice. *Psych. Rev.* 117(4):1275–1293.

Tversky A (1972) Elimination by aspects: A theory of choice. *Psych. Rev.* 79(4):281–299.

Tymula AA, Glimcher PW (2019) Expected Subjective Value Theory (ESVT): A representation of decision under risk and certainty. Working paper, University of Sydney, Sydney, Australia.

Vuong QH (1989) Likelihood ratio tests for model selection and nonnested hypotheses. *Econometrica* 57(2):307.

Wainwright MJ, Schwartz O, Simoncelli EP (2001) *Natural Image Statistics and Divisive Normalization: Modeling Nonlinearities and Adaptation in Cortical Neurons. Statistical Theories of the Brain* (MIT Press, Cambridge, MA).

Wang AY, Miura K, Uchida N (2013) The dorsomedial striatum encodes net expected return, critical for energizing performance vigor. *Nat. Neurosci.* 16(5):639–647.

Wasserman L (2000) Bayesian model selection and model averaging. *J. Math. Psych.* 44(1):92–107.

Webb R (2019) The (neural) dynamics of stochastic choice. *Management Sci.* 65(1):230–255.

Webb R, Levy I, Lazzaro S, Rutledge RB, Glimcher PW (2019) Neural random utility: Relating cardinal neural observables to stochastic choice behaviour. *J. Neurosci. Psych. Econom.* 12(1):45–72.

Weber E (1834) *On the Tactile Senses* [Trans. De Tactu] (Experimental Psychology Society, New York)

Weber EU, Johnson EJ (2009) Mindful judgment and decision making. *Ann. Rev. Psych.* 60(1):53–85.

Wei XX, Stocker AA (2017) Lawful relation between perceptual bias and discriminability. *Proc. Natl. Acad. Sci. USA* 114(38):10244–10249.

Wilcox NT (2011) 'Stochastically more risk averse:' A contextual theory of stochastic discrete choice under risk. *J. Econom.* 162(1):89–104.

Woodford M (2012) Prospect theory as efficient perceptual distortion. *Amer. Econom. Rev.* 102(3):41–46.

Yamada H, Louie K, Tymula A, Glimcher PW (2018) Free choice shapes normalized value signals in medial orbitofrontal cortex. *Nat. Comm.* 9(1):162.

Yoo SBM, Hayden BY (2018) Economic choice as an untangling of options into actions. *Neuron* 99(3):434–447.

Zimmermann J, Glimcher PW, Louie K (2018) Multiple timescales of normalized value coding underlie adaptive choice behavior. *Nat. Comm.* 9(1):3206.